Molecular Pharmacology Fast Forward. Published on February 26, 2013 as doi:10.1124/mol.112.083949

MOL #83949

Title: Probing the Metabotropic Glutamate Receptor 5 (mGlu5) Positive Allosteric Modulator (PAM) Binding Pocket: Discovery of Point Mutations that Engender a "Molecular Switch" in PAM Pharmacology

Karen J. Gregory, Elizabeth D. Nguyen, Sean D. Reiff, Emma F. Squire, Shaun R. Stauffer, Craig W. Lindsley, Jens Meiler and P. Jeffrey Conn.

Department of Pharmacology, Vanderbilt University Medical Center, Nashville, TN, USA (K.J.G., S.D.R., E.F.S., S.R.S., C.W.L., P.J.C.).

Vanderbilt Center for Neuroscience Drug Discovery, Vanderbilt University Medical Center, Nashville, TN, USA (K.J.G., S.D.R., E.F.S., S.R.S., C.W.L., P.J.C.).

Drug Discovery Biology, Monash Institute of Pharmaceutical Sciences, Monash University, Parkville, VIC, Australia (K.J.G.)

Center for Structural Biology, Vanderbilt University Medical Center, Nashville, TN, USA (E.D.N., J.M.)

Department of Chemistry and the Institute for Chemical Biology, Vanderbilt University Medical Center, Nashville, TN, USA (J.M.).

Copyright 2013 by the American Society for Pharmacology and Experimental Therapeutics.

Running Title: Mutations cause pharmacological switches in mGlu5 modulators

Corresponding Author:

P. Jeffrey Conn

1215 Light Hall

2215-B Garland Ave

Nashville, TN, USA

37232

Jeff.conn@vanderbilt.edu

Number of text pages: 50

Number of tables: 4

Number of figures: 10

Number of references: 58

Number of words in Abstract: 233

Number of words in Introduction: 750

Number of words in Discussion: 1531

Non-standard abbreviations: [^{3}H]methoxyPEPy, [^{3}H]-3-methoxy-5-(pyridin-2-ylethynyl)pyridine; 7TMRs, seven-transmembrane spanning (G protein-coupled) receptors; CaSR, Calcium-sensing receptor; CDPPB: 3-cyano-N-(1,3-diphenyl-1H-pyrazol-5-yl)benzamide; CPPHA, N-[4-Chloro-2-[(1,3-dioxo-1,3-dihydro-2H-isoindol-2-yl)methyl]phenyl]-2-hydroxybenzamide; DFB, difluorobenzaldazine; DMEM, Dulbecco's modified eagle medium; FBS, fetal bovine serum;

HTS, high-throughput screening; L-DOPA: L-3,4-dihydroxyphenylalanine; MCM, Monte Carlo Metropolis; mGlu, metabotropic glutamate receptor; MOE, Molecular Operating Environment; MPEP, 2-methyl-6-(phenylethynyl)-pyridine; NAM, negative allosteric modulator; PAM, positive allosteric modulator; PDB, Protein Data Bank; SAM: silent allosteric modulator; SAR, structure-activity relationship; VU0360172 (N-cyclobutyl-6-((3-fluorophenyl)ethynyl)nicotinamide hydrochloride), VU0360173, ((6-((3-fluorophenyl)ethynyl)pyridin-3-yl)(3-hydroxyazetidin-1-yl)methanone); VU0403602, (N-cyclobutyl-5-((3-fluorophenyl)ethynyl)ethynyl)picolinamide hydrochloride); VU0405386, N-(tert-butyl)-5-((3-fluorophenyl)ethynyl)picolinamide; VU0405398, (5-((3-fluorophenyl)ethynyl)pyridin-2-yl)(3-hydroxyazetidin-1-yl)methanone; VU0415051, N-tert-butyl-6-[2-(3-fluorophenyl)ethynyl]pyridine-3-carboxamide; VU29: 4-nitro-N-(1,3-diphenyl-1H-pyrazol-5-yl)benzamide.

Abstract

Positive allosteric modulation of metabotropic glutamate receptor subtype 5 ($mGlu_5$) is a promising novel approach for the treatment of schizophrenia and cognitive disorders. Allosteric binding sites are topographically distinct from the endogenous ligand-(orthosteric) binding site, allowing for co-occupation of a single receptor with the endogenous ligand and an allosteric modulator. Negative allosteric modulators (NAMs) inhibit, while positive allosteric modulators (PAMs) enhance, the affinity and/or efficacy of the orthosteric agonist. The molecular determinants that govern $mGlu_5$ modulator affinity versus cooperativity are not well understood. Focusing on the modulators based on the acetylene scaffold, we sought to determine the molecular interactions that contribute to PAM versus NAM pharmacology. Generation of a comparative model of the transmembrane-spanning region of $mGlu_5$ served as a tool to predict and interpret the impact of mutations in this region. Application of an operational model of allosterism allowed for determination of PAM and NAM affinity estimates at receptor constructs that possessed no detectable radioligand binding as well as delineation of effects on affinity versus cooperativity. Novel mutations within the transmembrane domain regions were identified that had differential effects on acetylene PAMs versus 2-methyl-6-(phenylethynyl)-pyridine (MPEP), a prototypical NAM. Three conserved amino acids (Y658, T780, S808) and two non-conserved residues (P654, A809) were identified as key determinants of PAM activity. Interestingly, we identified two point mutations in TM6 and 7 that, when mutated, engender a mode switch in the pharmacology of certain PAMs.

Introduction

Metabotropic glutamate receptors (mGlus) are seven-transmembrane spanning (G protein-coupled) receptors (7TMRs) that include eight subtypes, $mGlu_1$- $mGlu_8$, for the major excitatory neurotransmitter, glutamate (Niswender and Conn, 2010). Historically, it has been difficult to develop highly mGlu subtype selective ligands due to the high sequence conservation of the endogenous ligand (i.e., glutamate) orthosteric binding site. This led to the search for compounds that interact at "allosteric" sites, topographically distinct from the orthosteric site. Referred to as allosteric modulators, the presence of such compounds can affect the affinity and/or efficacy of an orthosteric ligand, a property referred to as cooperativity. Modulators that inhibit orthosteric ligand binding and/or activity are negative allosteric modulators (NAMs) while those that enhance are positive allosteric modulators (PAMs); a third category, silent (or neutral) allosteric modulators (SAMs), includes compounds that bind but do not modulate receptor activity.

Efforts to develop mGlu allosteric modulators have been especially successful for $mGlu_5$; a broad range of allosteric modulators as well as allosteric radioligands has been developed including pure PAMs, PAMs with agonist activity, weak and full NAMs and SAMs (Ametamey et al., 2007; Chen et al., 2007; 2008; Cosford et al., 2003; Gasparini et al., 1999; Honer et al., 2007; Kinney et al., 2005; Liu et al., 2008; Noetzel et al., 2012; O'Brien et al., 2004; Rodriguez et al., 2005; 2009; 2010; Treyer et al., 2007; Varney et al., 1999). $mGlu_5$ PAMs have potential utility for treatment of cognitive disorders and schizophrenia, whereas NAMs are being pursued for treatment of Fragile X Syndrome, depression, anxiety and L-DOPA-induced dyskinesia (Gregory et al., 2011).

In addition to improvements in receptor selectivity, allosteric modulators offer a number of theoretical advantages over their competitive counterparts (Melancon et al., 2012). Modulators

that possess no intrinsic efficacy have potential for spatial and temporal modulation of receptor activity. This is an especially important consideration for potential CNS therapeutics, where 'fine-tuning' neurotransmission is likely to yield a better therapeutic outcome than the sustained blockade or activation by an orthosteric ligand. Furthermore, the cooperativity between the two sites is saturable; thus, allosteric modulators have a built-in "ceiling level" to their effect, and may therefore have a larger therapeutic index in the case of overdose.

Structure-activity relationships (SAR) for mGlu modulators, particularly with respect to targeting $mGlu_5$, are also notoriously difficult; SAR is often 'steep' or 'flat' with minimal changes to the structure resulting in a complete loss of activity (Zhao et al., 2007). Furthermore, numerous mGlu modulator chemotypes display 'molecular switches' whereby a PAM or SAM arises from a NAM scaffold or vice versa (Wood et al., 2011); originally observed during discovery of the first $mGlu_5$ PAM, difluorobenzaldazine (DFB) (O'Brien et al., 2004). This phenomenon continues to be a challenge for medicinal chemists, with PAMs being derived from NAM scaffolds (Rodriguez et al., 2010; Sharma et al., 2009; Zhou et al., 2010), SAMs from either NAM or PAM chemotypes (Hammond et al., 2010; Rodriguez et al., 2005), and NAMs from PAMs (Lamb et al., 2011). Furthermore, molecular switches have also been described with respect to unanticipated alterations in receptor selectivity (Sheffler et al., 2012). Steep or flat SAR and "molecular switches" may be attributed to changes in the affinity and/or cooperativity of an allosteric modulator. Therefore, we were interested in probing the determinants of allosteric modulator affinity and cooperativity, focusing on the common allosteric site of group I mGlu's as previously identified for $mGlu_5$ selective modulators such as 2-methyl-6-(phenylethynyl)-pyridine (MPEP) (Malherbe et al., 2003; 2006; Muhlemann et al., 2006; Pagano et al., 2000). Two classes of acetylene PAMs, picolinamides and nicotinamides, that originally evolved from a

NAM high-throughput screen (HTS) lead (Rodriguez et al., 2010) were selected for in-depth characterization in comparison with MPEP. We identified seven novel residues that, when mutated, significantly decrease MPEP affinity. Moreover, a single point mutation (W784A) reduced the cooperativity of MPEP, such that it no longer fully blocked the response to glutamate. PAMs were found to interact with the common allosteric site utilized by MPEP, although these compounds showed differential sensitivities to certain mutations. Two different point mutations were identified that conferred a "molecular switch" in the pharmacology of PAMs: T780A converted N-tert-butyl-6-[2-(3-fluorophenyl)ethynyl]pyridine-3-carboxamide (VU0415051) to a weak NAM while S808A converted ((5-((3-fluorophenyl)ethynyl)pyridin-2-yl)(3-hydroxyazetidin-1-yl)methanone (VU0405398) from a weak PAM to a full NAM and N-(tert-butyl)-5-((3-fluorophenyl)ethynyl)picolinamide (VU0405386) from a PAM to a neutral modulator. Our findings build on the existing understanding of the location of the common allosteric site. Quantification of the effect of mutations on modulator pharmacology has allowed delineation of determinants for cooperativity versus affinity.

Materials and Methods

Materials

Dulbecco's Modified Eagle's Medium (DMEM), fetal bovine serum (FBS) and antibiotics were purchased from Invitrogen (Carlsbad, CA). [^{3}H]-3-methoxy-5-(pyridin-2-ylethynyl)pyridine ([^{3}H]methoxyPEPy; 76.3 Ci/mmol) was custom synthesized by PerkinElmer Life and Analytical Sciences (Waltham, MA). VU0360172 (N-cyclobutyl-6-((3-fluorophenyl)ethynyl)nicotinamide hydrochloride), VU0405398 ((5-((3-fluorophenyl)ethynyl)pyridin-2-yl)(3-hydroxyazetidin-1-yl)methanone), VU0405386 (N-(tert-butyl)-5-((3-fluorophenyl)ethynyl)picolinamide) and VU0415051 (N-tert-butyl-6-[2-(3-fluorophenyl)ethynyl]pyridine-3-carboxamide) were all synthesized in-house using previously reported methodologies (Gregory et al., 2012; Rodriguez et al., 2010). VU0360173 ((6-((3-fluorophenyl)ethynyl)pyridin-3-yl)(3-hydroxyazetidin-1-yl)methanone) and VU0403602 (N-cyclobutyl-5-((3-fluorophenyl)ethynyl)ethynyl)picolinamide hydrochloride) were synthesized in-house (Supplementary Materials S1). Unless otherwise stated, all other reagents were purchased from Sigma-Aldrich (St. Louis, MO) and were of an analytical grade.

Cell culture and mutagenesis

Mutations were introduced into the wild type rat $mGlu_5$ in pCI:Neo using site-directed mutagenesis (Quikchange II, Agilent, Santa Clara, CA) and verified by sequencing. Wild type and mutant rat $mGlu_5$ receptor constructs were transfected into HEK293A cells, using Fugene6^{TM} (Promega, Madison, WI) as the transfection reagent. Polyclonal stable cell lines were derived for rat $mGlu_5$ mutant constructs by maintaining the cells at sub-confluence for a minimum of four passages in the presence of 1 mg/ml G418 (Mediatech, Manassas, VA). Stably transfected cell

lines were subsequently maintained in complete DMEM supplemented with 10% fetal bovine serum (FBS), 2 mM L-glutamine, 20 mM HEPES, 0.1 mM Non-Essential Amino Acids, 1 mM sodium pyruvate, antibiotic-antimycotic and 500 μg/ml G418 at 37°C in a humidified incubator containing 5% CO_2, 95% O_2.

Intracellular Ca^{2+} mobilization

The day prior to assay, HEK293A-rat $mGlu_5$ cells were seeded at 50,000 cells/well in poly-D-lysine coated black-walled, clear bottom 96 well plates in assay medium (DMEM supplemented with 10% dialyzed fetal bovine serum, 20 mM HEPES and 1 mM sodium pyruvate). On the day of assay, the cell permeant Ca^{2+} indicator dye Fluo-4 (Invitrogen, Carlsbad, CA) was used to assay receptor-mediated Ca^{2+} mobilization as described previously (Hammond et al., 2010) using a Flexstation II (Molecular Devices, Sunnyvale, CA). A 5-point smoothing function was applied to the raw fluorescent Ca^{2+} traces and basal fluorescence of individual wells determined during the first 20 sec. The peak increase in fluorescence over basal was determined prior to normalization to the maximal peak response elicited by glutamate.

Radioligand binding

Radioligand binding assays were performed on HEK293A cell membranes as described previously (Gregory et al., 2012). Briefly, for saturation binding experiments, membranes (20-50 μg/well) were incubated with a range of [^{3}H]methoxyPEPy concentrations (0.5 nM-60 nM) for 1 hr at room temperature with shaking in Binding Buffer (50 mM Tris-HCl, 0.9% NaCl, pH7.4). 10 μM MPEP was used to determine non-specific binding. For inhibition binding experiments, membranes were incubated with ~2 nM [^{3}H]methoxyPEPy and a range of concentrations of test

ligand (100 pM-100 μM) for 1 hr at room temperature with shaking in Ca^{2+} assay buffer with 1% DMSO final. Assays were terminated by rapid filtration through GF/B Unifilter plates (PerkinElmer Life and Analytical Sciences, Boston, MA) using a Brandel 96-well plate Harvester (Brandel Inc., Gaithersburg, MD), and three washes with ice-cold Binding Buffer, separating bound from free radioligand. Plates were allowed to dry overnight and radioactivity counted using a TopCount Scintillation Counter (PerkinElmer Life and Analytical Sciences, Boston, MA).

Generation of an $mGlu_5$ comparative model

A comparative model of $mGlu_5$ was constructed using the protein structure prediction software package, Rosetta version 3.4 (Leaver-Fay et al., 2011). Based on its high similarity (e-value of 3e-15 with a sequence coverage of 90%) to $mGlu_5$ according to a search using NCBI BLASTP on sequences from the Protein Data Bank (PDB), the X-ray crystal structure human β_2-adrenergic receptor (PDB ID: 2RH1) (Cherezov et al., 2007) was chosen as a template. Both β_2-adrenergic receptor and $mGlu_5$ also share a conserved disulfide bond between a cysteine at the top of transmembrane helix three and a cysteine in extracellular loop two. Members of the Family C 7TMRs, namely the human mGlus and Calcium-sensing receptor (CaSR) sequences, were first aligned with CLUSTALW. Alignment of TM regions between Family C 7TMRs and Family A crystal structure templates were directly adopted from (Malherbe et al., 2006), with the exception of TM's 2, 4 and 7, which were based on the alignment of CaSR with Family A 7TMRs from (Miedlich et al., 2004)(Supplementary Fig. S1). In the construction of the comparative models, the backbone coordinates of the β_2-adrenergic receptor were retained in the comparative model of $mGlu_5$ while the loop coordinates were built in Rosetta using Monte Carlo Metropolis (MCM) fragment replacement combined with cyclic coordinate descent loop closure. Rosetta ensures that

ϕ-ψ angles of backbone segments from homologous sequence fragments from the PDB are introduced into the loop regions. After the fragment substitution, small movements in the ϕ-ψ angles are performed to close breaks in the protein chain. The resulting full sequence models were subjected to eight iterative cycles of side chain repacking and gradient minimization of ϕ, ψ and χ angles in Rosetta Membrane (Yarov-Yarovoy et al., 2006).

Docking of allosteric modulators

The negative allosteric modulator MPEP and six acetylene PAMs (VU0360173, VU0405398, VU0360172, VU0403602, VU0415051 and VU0405386) were computationally docked into the comparative model of $mGlu_5$ using Rosetta Ligand (Davis and Baker, 2009; Lemmon and Meiler, 2012; Meiler and Baker, 2006). Each modulator was allowed to sample docking poses in a 5 Å radius centered at the putative binding site for MPEP, determined by the residues known to affect modulator affinity and/or function. For MPEP, separate docking experiments were carried out, centered on two residues shown to greatly influence modulator affinity when mutated: P654 and S808. For the six acetylene PAMs, docking experiments were all centered on P654. Once a binding mode had been determined by the docking procedure, 10 low energy conformations of the ligand created by MOE (Molecular Operating Environment, Chemical Computing Group, Ontario, Canada) were tested within the site. Side-chain rotamers around the ligand were optimized simultaneously in a Monte-Carlo minimization algorithm. The energy function used during the docking procedure contains terms for van der Waals attractive and repulsive forces, hydrogen bonding, electrostatic interactions between pairs of amino acids, solvation, and a statistical term derived from the probability of observing a side-chain conformation from the PDB. For each modulator, over 2,000 docked complexes were generated and clustered for

structural similarity using bcl::Cluster (Alexander et al., 2011). The lowest energy binding mode from the five largest clusters for each modulator were used for further analysis. A detailed protocol capture for protein modeling and ligand docking, including links to input and output files, is provided (Supplementary Materials S2; Supplementary Materials S3).

Data Analysis

All computerized nonlinear regression was performed using Prism 5.01 (GraphPad Software, San Diego, CA). Inhibition [^{3}H]methoxyPEPy binding data sets were fitted to a one-site inhibition binding model and estimates of inhibitor dissociation constants (K_I) were derived using the Cheng-Prusoff equation for competitive ligands (Cheng and Prusoff, 1973) and the following version of the allosteric ternary complex model for ligands that did not fully displace radioligand (Lazareno and Birdsall, 1995):

$$\frac{Y}{Y_{max}} = \frac{[D]}{[D] + \frac{K_D\left(1+\frac{[B]}{K_B}\right)}{\left(1+\frac{\alpha[B]}{K_B}\right)}}$$

where Y/Y_{max} is the fractional specific binding, D is the radioligand concentration, B is the molar concentration of the allosteric modulator, K_D is the radioligand equilibrium dissociation constant, and K_B is the allosteric modulator equilibrium dissociation constant. α denotes the cooperativity factor, where values of $\alpha > 1$ describe positive cooperativity, values of $\alpha < 1$ (but greater the 0) denote negative cooperativity and $\alpha = 1$ denotes neutral cooperativity.

Shifts of glutamate concentration-response curves by allosteric modulators were globally fitted to an operational model of allosterism (Leach et al., 2007):

$$Effect = \frac{E_m(\tau_A A(K_B + \alpha\beta B) + \tau_B B K_A)^n}{(AK_B + K_A K_B + K_A B + \alpha AB)^n + (\tau_A A(K_B + \alpha\beta B) + \tau_B B K_A)^n}$$

where A is the molar concentration of orthosteric agonist glutamate and B is the molar concentration of the allosteric modulator. K_A is the equilibrium dissociation constant of the orthosteric agonist, glutamate, and K_B is the allosteric modulator equilibrium dissociation constant.

Affinity modulation is governed by the cooperativity factor α, and efficacy modulation is governed by β. The parameters τ_A and τ_B relate to the ability of the orthosteric and allosteric ligands, respectively, to engender receptor activation. E_m and *n* denote the maximal possible system response and the transducer function that links occupancy to response, respectively.

Allosteric modulator and agonist concentration-response curves were fitted to a four parameter logistic equation in order to determine potency estimates:

$$y = \frac{bottom + (top - bottom)}{(1 + 10^{(logEC_{50} - A)HillSlope}}$$

where *bottom* and *top* are the lower and upper plateaus, respectively, of the concentration-response curve, HillSlope is the Hill coefficient that describes the steepness of the curve, and EC_{50} is the molar concentration of modulator required to generate a response halfway between the *top* and *bottom*.

All affinity, cooperativity and potency parameters were estimated as logarithms and are expressed as the mean ± S.E.M. (Christopoulos, 1998). Statistical analyses were performed where appropriate as indicated using one-way ANOVA with Dunnett's post test when comparing to control, or Tukey's post-test when making multiple comparisons.

Results

Refining the alignment of $mGlu_5$ to Family A 7TMRs and prediction of amino acids within the common allosteric "MPEP" site

In contrast to previous models of $mGlu_5$ (Malherbe et al., 2006; Malherbe et al., 2003; Pagano et al., 2000), the alignment of $mGlu_5$ presented here is based on a previously reported CaSR alignment (Miedlich et al., 2004) where the PKxY motif in transmembrane domain 7 (TM7) of the human mGlus is aligned with the NPxxY motif in the Family A 7TMRs (Supplementary Fig. 1). This adjustment in the alignment shifts TM7 by seven residues, predicting that S806, S808 and T810 face the MPEP binding pocket. Indicated on the alignment of the human mGlus with bovine rhodopsin and human β_2-adrenergic receptor (Supplementary Fig. 1) are point mutations included in the current study, which includes mutations previously reported to perturb NAM or PAM activity of $mGlu_5$ modulators (Chen et al., 2008; Malherbe et al., 2006; Malherbe et al., 2003; Molck et al., 2012; Muhlemann et al., 2006; Pagano et al., 2000) and mutations novel to this study (highlighted in grey). Based on the localization of these previously known residues, we elected to mutate additional residues predicted to be on the same inward-facing helical face of TMs 3, 5, 6 (I650A, G651F, V739M, P742S, N746A, G747V, T779A, I783A, V788A, Y791F, F792A). Conserved residues were substituted for Ala, whilst non-conserved residues were mutated to the corresponding amino acid in either group II or group III mGlus. In order to validate the alignment of TM7, seven residues were mutated that were predicted to line the inward-facing helical face of TM7: S806A, S808A, S808T, T810A, T810S, A812S, L813A, C815A, M816A. As a negative control, a point mutation previously shown to affect PAM activity (by CPPHA) at the second allosteric site on $mGlu_5$, F585I, was also included (Chen et al., 2008).

Identification of eight novel point mutations that perturb MPEP inhibition of glu

To assess the contribution of both novel and previously identified residues to the MPEP binding pocket, MPEP (Fig. 1) was screened for its effect on the maximal response to glutamate in the Ca^{++} mobilization assay at a single concentration. For screening purposes 10 nM MPEP was selected as this concentration caused a significant decrease in glutamate E_{max} to ~45% at $mGlu_5$-wt, such that increases or decreases in the % inhibition caused by MPEP could be detected (Fig. 1A). All mutations were functional and expressed at levels ranging from 0.4-3.8 pmol/mg (Table 1, Supplementary Table 1). Mutations that showed a lack of [^{3}H]methoxyPEPy binding showed a similar range of expression levels (between that of the low-expressing $mGlu_5$-wt cell line and the higher-expressing, polyclonal $mGlu_5$-wt line) as confirmed by immunoblotting (Supplementary Fig. 2). Twelve point mutations, corresponding to nine different amino acids, significantly reduced inhibition of glu E_{max} by 10 nM MPEP (Fig. 1B). From the original 33 point mutations screened, 24 were selected for further characterization, including the negative control F585I.

Delineation of impact of mutations on MPEP affinity versus cooperativity

Progressive fold-shift analysis by MPEP of the glutamate concentration-response curve for Ca^{++} mobilization was performed using the operational model of allosterism (Leach et al., 2007). This model has previously been validated for estimating affinity and cooperativity of $mGlu_5$ allosteric modulators (Gregory et al., 2012). As expected, given that mutations were introduced into the TMs, little or no change was observed in the potency and efficacy ($\log\tau_A$) of glutamate across all point mutations compared to wild type (Supplementary Table 1).

Furthermore, the assumption that glutamate affinity was unaffected by point mutations in the TMs had no effect on the estimates of modulator pK_B (Supplementary Fig. 1A). The affinity (pK_B) of MPEP was found to be significantly reduced compared to wild type at 16 point mutations (Table 1, Fig. 1C). MPEP affinity estimates were reduced 3-10 fold at: P742S, L743V, G747V, T779A, V788A and T810A; 10-30 fold at G651F, P654S, T780A and A809G; 30-100 fold at Y658V, S808A, S808T and A809V. Greater than 1000-fold lower MPEP affinity was observed at P654F and W784A compared with wild type. Binding and functional affinity estimates showed good agreement. No appreciable [^{3}H]methoxyPEPy binding was observed at G651F, P654S, P654F, Y658V, T780A, W784A, S808A, S808T, A809V and A809G (Table 1), corresponding to mutations where MPEP affinity was estimated to be decreased 10 fold or greater compared to wild type. MPEP completely blocked the maximal response to glutamate at all constructs (data not shown) with the exception of P654F and W784A (Fig. 2A & B). At W784A (Fig. 2B), inhibition of glutamate by MPEP approached a limit, where $\log\beta = -0.27\pm0.03$, indicating that MPEP negative cooperativity is weaker at W784A compared to wild type.

Modeling MPEP binding to mGlu$_5$ comparative model

MPEP was docked into the comparative model of $mGlu_5$ to aid interpretation of these mutational data. Docking experiments were centered on two sites, represented by two residues that were demonstrated to reduce MPEP affinity when mutated, P654 and S808. Representative binding modes from each experiment demonstrate possible binding modes for MPEP interacting with $mGlu_5$ (Fig. 3A). The lowest energy MPEP binding poses from the largest clusters for docking to both sites are shown in Fig. 3B and 3C. Docking to P654 identified a common binding site within the top three clusters, representing 37% of all models; five out of seven point

mutations that reduce MPEP affinity are predicted to line the pocket depicted by these poses. However, given the linearity of MPEP, the orientation of the ligand proved more difficult for Rosetta to differentiate; in two of the top three clusters the pyridine ring of MPEP points towards the extracellular space. Interestingly, despite mutations causing 30-100 fold reduction in affinity, S808 and A809 were not predicted to interact with MPEP in the P654-based docking runs. The lowest energy MPEP binding modes of the largest five clusters (accounting for 28% of models) with docking centered on S808 demonstrated greater diversity (Fig. 3B). In four out of these five binding modes, the nitrogen from the pyridine ring forms a hydrogen bond with S808. A similar pose for MPEP has recently been reported (Molck et al., 2012). This interaction may also account for the impact of substitutions to A809, potentially influencing the conformation of its neighboring residue S808. Given the location of S808 at the top of TM7 closer to extracellular loop regions, the greater diversity in binding poses is not unreasonable. We hypothesize that S808 and A809 are important for the initial recognition of the receptor by MPEP, ultimately facilitating binding deeper within the pocket created by TMs 3, 5, 6 and 7. Residues that when mutated significantly reduced MPEP affinity are highlighted in Fig. 3 and color-coded based on their relative impact on MPEP affinity. Notably, residues that have the greatest effect on MPEP affinity are found in close proximity to MPEP, whereas as those with less of an effect (3-10 fold reduction) are more remote. Hydrophobic interactions with MPEP are likely occurring with W784 and Y658. Given its placement in relation to MPEP, the P654F mutation may introduce steric clash into the MPEP binding site preventing MPEP binding and consequently reducing affinity. Ser substitution of this same amino acid did not reduce affinity to the extent of the Phe mutation, with MPEP negative cooperativity retained. Thus it is also possible that replacing Pro with Phe both influences the helix conformation (by removing Pro induced kink) and introduces a larger

hydrophobic amino acid, thereby dramatically changing the geography of the MPEP binding pocket, perturbing MPEP affinity and potentially cooperativity. The effect of mutations to S806, S808 and T810 provide evidence in favor of the alignment of the PKxY motif in the mGlus with NPxxY motif in the Family A 7TMRs. As predicted by the model, the S808A mutation affects MPEP affinity, likely because its position facing the binding pocket provides an interaction with MPEP. S806 and T810 face away from the binding pocket and are not predicted to affect affinity, which is in agreement with the functional data (Fig. 1C). This verification of the MPEP binding mode through point mutations encouraged the further analysis with positive allosteric modulators of $mGlu_5$.

Identification of point mutations that affect positive allosteric modulation of glu activity

Three pairs of picolinamide and nicotinamide acetylene $mGlu_5$-selective positive allosteric modulators were selected for investigation of the binding mode of these two chemical scaffolds in the common allosteric site of $mGlu_5$ (Fig. 4). These six PAMs span varying degrees of affinity at the wild type receptor from low (VU0360173, 8 μM) to high (VU0403602, 6 nM; VU0405386, 10 nM) (Tables 2 & 3). Picolinamide PAMs show higher affinity ~10 fold for the wild type receptor than their nicotinamide counterparts (Tables 2 & 3). Furthermore, these PAMs show varying degrees of cooperativity, i.e. their ability to induce leftward shifts (fold-shifts) of the glutamate concentration-response curve (Fig. 4; Table 4). Similar to the approach utilized for MPEP above, activity of mutant receptors was assessed at a single concentration of PAM. Based on the ability of these compounds to potentiate glutamate Ca^{++} mobilization at the wild type receptor (Fig. 4), PAM concentrations were selected that caused sub-maximal, but reproducible, fold-shifts in the concentration-response curve to glutamate. The fold-shift at a single

concentration of PAM was compared with the fold-shift at wild type (Fig. 5). Point mutations that significantly increased or decreased potentiation were selected for further characterization using analysis of progressive fold-shift of the glutamate concentration-response curve to delineate their effects on PAM affinity versus cooperativity.

Impact of mutations on PAM affinity: interactions within the common allosteric pocket

To ensure that potential determinants were not missed in the initial screen, mutations that perturbed potentiation by at least one member of class (either picolinamide or nicotinamide) were assessed across all three members. In addition, mutations that affected one member of a picolinamide/nicotinamide PAM pair were further assessed at both. Affinity estimates (pK_B) for PAMs, derived from modulation of glutamate- mediated Ca^{++} mobilization, are shown in Table 3; for the most part, mutations influenced modulator affinity (Fig. 6). Where practical, PAM affinity was also assessed using inhibition of [^{3}H]methoxyPEPy binding (Table 2). Functional (pK_B) and binding (pK_I) estimates of affinity showed strong correlation (Supplementary Fig. 3B). All mutations in TM3 that showed significant effects could not be assessed using radioligand binding-based approaches, relying instead on affinity estimates derived using the operational model of allosterism.

No potentiation was evident for VU0360173 (up to 30 μM) at G651F, P654S, P654F, Y658V, T780A, S808A, and A809V. The corresponding picolinamide, VU0405398, also showed no detectable potentiation at A809V and 10-30 fold decreased affinity at G651F, P654S, T780A and A809G; 30-100 fold reductions were noted at P654F and Y658V. Collectively, these results suggest that the lack of potentiation observed for VU0360173 at these mutants is a result of decreased affinity.

VU0360172 affinity was reduced approximately 10 fold at G651F and A809V. No positive allosteric modulation was observed at Y658V or T780A. Interestingly, P654S had no significant effect on VU0360172 affinity, while at the Phe substitution VU0360172 affinity was also reduced (6 fold; this did not reach significance). The picolinamide counterpart of VU0360172, VU0403602, also showed no appreciable PAM activity at Y658V, alongside marked reductions in affinity (greater than 100 fold) at P654F and T780A. VU0403602 affinity was also decreased 30-100 fold at G651F, S808A, A809V and A809G; and 10-30 fold at S808T. At P654S and C815A, VU0403602 pK_B values were reduced 3-10 fold compared to wildtype; although this did not reach significance at P654S.

Similar to that reported for the previous four PAMs, VU0415051 did not potentiate glutamate at Y658V (up to 30 μM). Decreased VU0415051 affinity was noted at: S808T, A809G (10-30 fold); P654S, T780A, A809V (30-100); and greater than 100 fold at P654F. VU0405386 also showed no discernible PAM activity at Y658V nor S808A. The affinity of VU0405386 was decreased compared to wildtype at F792A, A809G (10-30 fold); P654F, A809V (30-100 fold); and greater than 300 fold at T780A. Interestingly, neither of the VU0415051/VU0405386 pair were unaffected by G651F.

Three point mutations in TM5, P742S, L743V and N746A, showed no significant effects in functional assays; however, in inhibition binding assays, significant reductions in affinity were observed for some PAMs (Table 2). P742S significantly decreased pK_I values 3-10 fold for VU0361072, VU0403602, VU0415051 and VU0405386. Significantly decreased pK_I values were also noted for VU0403602 (19 fold), VU0405398 (2 fold), VU0415051 (4 fold) at L743V, and for VU0403602 (6 fold), VU0415051 (3 fold) at N746A. In contrast, V788A, in TM6, showed a trend for increased pK_B and pK_I values (2-10 fold).

Docking of PAMs to mGlu$_5$ comparative model

Docking of the positive allosteric modulators in the mGlu$_5$ comparative model provides insight into the significant residues identified to reduce affinity in the binding pocket. Each of the six positive allosteric modulators were allowed to explore a 5 angstrom radius around P654, and the lowest energy binding modes of the largest 5 clusters were shown to bind in the same pocket as MPEP (Fig. 7A-C). As seen with MPEP, mutation of P654 in TM3 to a bulky residue (Phe) likely introduces a steric clash, reducing the ability of PAMs to engage the common mGlu$_5$ binding pocket, accounting for the reduced affinity for all six PAMs. As noted previously, the amino acid in this position in not conserved across the mGlu family, such that it is likely P654 also contributes to the subtype selectivity of these PAMs. Introduction of steric bulk is also likely to underscore the impact of the G651F mutation on all modulators except for the VU0415051/VU0405386 pair. The impact of substitution of Y658 with Val can likely be attributed to disruption of key polar interactions between modulators and Y658, T780 and W784 (Highlighted by dashed lines in Fig. 7A-C). Similarly, T780 likely participates in a polar interaction with the carbonyl of the PAMs, with the exception of VU0403602 where the tertiary amide is predicted to interact with this residue, such that Ala substitution of this amino acid causes the drastic loss of affinity seen for all modulators. W784 likely contributes to hydrophobic interactions within the pocket, which may account for the trend for picolinamide PAM affinity to be perturbed by W784A; it is also noteworthy that the W784 may be involved in a hydrogen bonding network linking the modulators, TM3 and TM7. V788A shows a trend for increased affinity, which may be due to secondary effects on protein conformation and the previously implicated F787, where Ala substitution reduced NAM and PAM interactions (Malherbe et al.,

2006; Malherbe et al., 2003; Muhlemann et al., 2006). S808 in TM7 may participate in hydrogen bonding with the fluorine of the modulators when in close proximity, although this was not evident in the lowest energy binding poses. Substitution of A809 with Gly or Val reduced modulator activity across the board, pointing to the importance of the alanine in maintaining the correct helix conformation for binding. With respect to C815 and VU0403602, it is likely that there is an interaction with the cyclobutane of the modulator; however, it is not immediately apparent whether this is a direct or indirect effect.

Quantifying effects on cooperativity: identification of mutations that engender "molecular switches"

When applying the operational model of allosterism, the interaction between glutamate and PAMs was assumed to be exclusively via efficacy modulation, an assumption previously validated for $mGlu_5$ PAMs from this scaffold (Gregory et al., 2012). Cooperativity estimates (logβ) are summarized in Table 4 and comparisons with wild type are shown in Fig. 8. Alongside marked reductions in PAM affinity, P654F also significantly increased cooperativity of VU0415051 (~2 fold). P742S in TM5 had no effect on PAM affinity, yet increased cooperativity (~3 fold). In TM7, A809G significantly increased the cooperativity of the higher affinity PAMs: VU0403602, VU0415051 and VU0405386 (2-5 fold), with a similar trend observed for VU0360172, VU0360173 and VU0405398. Also in TM7, C815A significantly increased the cooperativity of all PAMs (2-7 fold) with the exception of VU0405398. P742S, A809G, C815A all represent mutations where the glutamate potency and/or efficacy was lower than the wild type (Supplementary table 1), such that these increases in PAM cooperativity may be attributable to PAMs stabilizing an unstable mutant receptor. Significantly increased cooperativity (3 fold) was

also observed at W784A for VU0360172, VU0403602 and VU0415051, with VU0360173 showing higher, although not significant, cooperativity. Interestingly, this was not a global PAM phenomenon as the cooperativity of VU0405386 and VU0405398 unchanged. Given the putative involvement of W784 in a key hydrogen bonding network for the PAMs (dotted lines in Fig. 7A-C), perhaps this differential effect is driven by the relative importance of this interaction over that of the PAM functional head group. Also in TM6, V788A increased the cooperativity of VU0360173 (3 fold) alone; no direct interaction is predicted from the docking between VU0360173 and V788, suggesting this is an indirect effect on the geography of the binding pocket. The selective effect of V788A on VU0360173 cooperativity may be attributable to the fact that this PAM has the weakest cooperativity and lowest affinity.

Three point mutations altered cooperativity drastically, such that PAMs behaved as NAMs. At Y658V, VU0405398 was a weak NAM, reducing the maximal response to glutamate by ~25% at 30 μM (Fig. 9A). This same mutation resulted in a loss of potentiation by all other PAMs. At T780A, VU0415051 became a weak NAM or "partial antagonist", where $\log\beta = -0.28$, corresponding to ~40% depression in the glutamate maximal response (Fig. 9B). This inhibition approached saturation, the hallmark feature of an allosteric interaction.

The most profound molecular switch engendered by a single point mutation was that of S808A, where VU0405398 behaved as a full NAM, abolishing the maximal response to glutamate (Fig. 9C). As mentioned earlier, at this same mutation VU0405386 showed no discernible PAM activity. Given that this mutation has little or no impact on the affinity of the other PAMs tested, we hypothesized that the lack of potentiation by VU0405386 was caused by a molecular switch from PAM to neutral. To test this hypothesis, concentration response curves for VU0405398 inhibition of an EC_{80} glutamate concentration were performed at S808A in the

presence of varied concentrations of VU0405386. As shown in Fig. 9D, VU0405386 has no effect on the response to glutamate, but causes parallel rightward shifts in the VU0405398 curve, in a manner consistent with a competitive interaction (Fig. 9E; where the Schild slope was not significantly different from unity (0.92 ± 0.09) and pK_B: 7.48 ±0.20).

Modeling PAM molecular switches

To investigate the molecular cause of the PAM to NAM or neutral switches, modulators were docked into $mGlu_5$ models containing the mutation engendering the switch. VU0405398 docked in wildtype $mGlu_5$ was compared to VU0405398 docked into the S808A mutant (Fig. 10A). Interestingly, introducing this single point mutation resulted in movement of TM7, such that in the mutant receptor VU0405398 is further away from this helix. It is unclear as to why this substitution results in such a conformational change of the receptor. Although not evident in the docked results, it is possible that rotation of the side chain of S808 in the wildtype receptor would allow hydrogen bonding to occur between the fluorine of the modulator and S808, with direct interactions with TM7 being important for stabilizing active receptor conformations. At the mutant receptor, such an interaction is no longer available and VU0405398 instead stabilizes an inactive receptor conformation at the mutated receptor. From the docked poses it is also evident that the picolinamide functional group of VU0405398 adopts a strikingly different orientation within the pocket. Similarly, VU0415051 was docked into the T780A mutant receptor and binding modes compared with those in wildtype $mGlu_5$ (Fig. 10B). At the T780A mutant, a polar interaction is no longer formed between the carbonyl of the modulator and the mutant A780; hydrogen bonding is no longer evident with the side chain hydroxyl of Y658 and the modulator carbonyl, nor between the tertiary nitrogen and S657. In the mutant receptor construct, the

nicotinamide tertbutyl moiety of VU0415051 adopts a different orientation with decreased affinity. Docking of VU0405386 in the S808A receptor shows subtle differences in the binding mode of the ligand when compared with wildtype (Fig. 10C). The movement of TM7 observed with docking VU0405398 to this same receptor mutation is not evident, which may account for the switch from PAM to neutral rather than to a robust NAM as seen for VU0405386. Although not evident in the static docked pose, we hypothesize that the side chain of S808 may rotate to form a polar interaction with the fluorine of the modulator when interacting with the wildtype receptor that is not possible in the mutant. It is also clear that this point mutation at the top of TM7 results in the ligand adopting a different pose with respect to the picolinamide tertbutyl group, which may contribute to the observed switch to neutral cooperativity.

Discussion

By utilizing an operational model of allosterism (Gregory et al., 2012; Leach et al., 2007), we have quantitatively assessed the interactions of positive allosteric modulators within the common allosteric site of $mGlu_5$, successfully delineating the impact of point mutations on cooperativity versus affinity. Seven novel point mutations were discovered that negatively impact the MPEP affinity, building on our understanding of the common allosteric binding pocket. Furthermore, Ala substitution of W784 reduced MPEP negative cooperativity. For the six PAMs studied, three conserved (Y658, T780, S808) and two non-conserved residues (P654, A809) were identified as critical determinants of PAM affinity. Interestingly, two point mutations engendered molecular switches in certain PAMs, changing their pharmacology to either NAMs or neutral modulators.

Close examination of the MPEP mutational data reveals a number of interesting observations. First, [^{3}H]methoxyPEPy non-binding mutants corresponded to mutations where MPEP affinity estimates, as derived from functional assays, were decreased 10 fold or greater compared to wildtype. Indeed, four previously reported mutations: Y658V, W784A, A809V, and A809G, that cause a loss of NAM binding to $mGlu_1$ and $mGlu_5$ and/or decreased MPEP potency for glutamate inhibition (Malherbe et al., 2003; 2006; Molck et al., 2012; Muhlemann et al., 2006; Pagano et al., 2000) were confirmed herein and attributed to >30 fold reductions in MPEP affinity. Also in agreement with previous data (Malherbe et al., 2003; 2006; Pagano et al., 2000), P654S, L743V and T780A all reduced MPEP affinity, although the effect of T780A was more pronounced in the current study than previously reported (17 versus 5 fold; (Malherbe et al., 2003)). Second, in mutating residues predicted to line the helical face towards the binding site as shown in the comparative model, we have further validated utilization of Family A 7TMR crystal

structures as templates for mGlu transmembrane spanning domain comparative modeling. Our TM7 alignment, aligns PKxY of $mGlu_5$ to the conserved NPxxY motif, differs by seven residues compared to earlier reports (Malherbe et al., 2006; Pagano et al., 2000), agreeing with the recent report by Molck and colleagues (Molck et al., 2012). In support of this new alignment for TM7, S808 was hypothesized to contribute to the common allosteric site of $mGlu_5$ as opposed to S806 and T810. Mutation of S808 to Ala perturbed MPEP affinity significantly more than S806A and T810A. S808T had a similar impact on MPEP affinity, suggesting a polar interaction may occur between S808 and MPEP that is not achieved by Thr. Alternatively, S808 may be important for maintaining the allosteric binding pocket geography, perhaps via a hydrogen bonding network.

Molecular models of receptor-ligand complexes provide important tools for hypothesis generation, predicting binding modes where experimental structures are unavailable. In the current study, the model provides an orientation of transmembrane helices, known to be aligned well across GPCR templates, as well as the TM7 helix/loop transition, that reasonably explains experimental results demonstrated by S806, S808 and T810 mutations. The comparative model has less confidence predicting receptor loop regions, as these have less than 20% sequence homology to the template GPCR structures used. The predicted modulator binding site captures residues identified in experimental studies, lending confidence to the binding site location depth within the receptor. The long axes of the ligands were consistently aligned parallel with the helices; however, computationally it was difficult predicting the orientation of these linear ligands and distinguishing whether the functional group points towards the intracellular or extracellular space. Despite these challenges, the $mGlu_5$ computational model with allosteric modulators has provided valuable hypotheses, validated experimentally herein.

Comparison of the PAM data with that of MPEP shows a number of marked differences in mutation susceptibility. Interestingly, more mutations perturbed MPEP affinity than the PAMs; however, with one exception (VU0403602 at C815A), there were no mutations that influenced PAM affinity without affecting MPEP. It is clear that these acetylene PAMs interact with the common allosteric site on $mGlu_5$. These differences likely underscore the determinants that contribute to a NAM versus PAM interacting with the receptor. Interestingly, W784A caused a ~1000 fold reduction in MPEP affinity; however, nicotinamide PAMs were insensitive to this mutation, whilst the picolinamides showed 3-10 fold decreased affinity. W784A increased cooperativity of some PAMs; in agreement with the previous report that W784A enhanced DFB potentiation (Muhlemann et al., 2006). Ala substitution of the equivalent Trp in $mGlu_1$ (W798) has differential effects on $mGlu_1$ NAMs (Fukuda et al., 2009; Suzuki et al., 2007). W784 is analogous to the W of the CWxP motif in Family A 7TMRs that is involved in the well-known rotamer-toggle activation switch (Holst et al., 2010; Shi et al., 2002; Visiers et al., 2002). The modeling herein predicts a network of polar interactions involving W784 and T780 in TM6, Y658 in TM3 and the PAMs. We hypothesize that the differential effect of W784A on $mGlu_5$ PAMs versus MPEP is likely underscored by PAMs interacting with an active versus inactive receptor conformation.

In each case, picolinamide modulators have higher affinity than their corresponding nicotinamide modulators. From the studies herein, it is not entirely clear which interactions within the binding pocket drive this higher affinity for picolinamides. However, a trend was observed where a greater reliance upon residues in TM7 was observed for compounds, both nicotinamides and picolinamides, with higher affinity (sub 100 nM). Picolinamides also tended to be susceptible to W784A; however, this only reached significance for VU0403602.

For all PAMs, Y658V abolished potentiation, except for VU0405398 where a weak NAM switch was observed. Trp substitution of the equivalent residue in $mGlu_8$ suppresses the activity of a constitutively active mutant receptor (Yanagawa et al., 2009), raising the possibility that this $mGlu_5$ mutation may have a global receptor activation effect. However, previously DFB potentiation was reportedly unaffected by Y658V (Muhlemann et al., 2006); supporting the hypothetical modulator binding modes shown, where an interaction is predicted with this residue, rather than Y658V impacting active receptor states.

A number of previous studies have identified PAMs as competitive with the common $mGlu_5$ allosteric (or "MPEP") site on the basis of a single point mutation in TM7, A809V (Chen et al., 2008; Hammond et al., 2010). Previously, A809V was reported to cause a ~30 fold decrease in the affinity of 4-nitro-N-(1,3-diphenyl-1H-pyrazol-5-yl)benzamide (VU29), an $mGlu_5$ PAM from the 3-cyano-N-(1,3-diphenyl-1H-pyrazol-5-yl)benzamide (CDPPB) series (Gregory et al., 2012). Validating the utilization of this single point mutation as a read-out of interaction with this common allosteric site, all six PAMs exhibited decreased affinity for this mutant construct. While this interaction appears to be crucial for all PAMs that are competitive with MPEP tested to date, it should be noted that this does not necessarily have to be the case. Notably, L743V and the equivalent mutation in $mGlu_1$ were previously shown to enhance potentiation by PAMs (Knoflach et al., 2001; Muhlemann et al., 2006); however, for acetylene PAMs, L743V had no effect on cooperativity or affinity. Further studies are underway to probe interactions within the common allosteric site by modulators from distinct chemotypes to better inform our understanding of the molecular determinants of modulator affinity and cooperativity (Manka et al., 2012).

A key finding arising from this study was the identification of residues that, when mutated, engendered a mode switch in allosteric modulator pharmacology, specifically T780A in TM6 and S808A in TM7. Considering that these PAMs originated from a NAM HTS lead (Rodriguez et al., 2010), such drastic changes in modulator cooperativity are not altogether surprising. Indeed, the acetylene series of mGlu allosteric modulators is prone to "molecular switches" (Wood et al., 2011); the SAR plagued by unanticipated changes in the mode of pharmacology and selectivity (Sheffler et al., 2012; Wood et al., 2011). Muhlemann and colleagues previously reported a similar result for the early $mGlu_5$ PAM, DFB, where at the F787A mutant, DFB behaved as a weak NAM (Muhlemann et al., 2006). Pharmacological mode switches were also noted during the discovery of DFB and related compounds (O'Brien et al., 2003). As noted above, movements in TM6 have been implicated in the transition of Family A 7TMRs from inactive to active states. TM7 contains the NPxxY motif, also well-known for its role in receptor activation (Barak et al., 1995; Fritze et al., 2003; Prioleau et al., 2002). Furthermore, a water-hydrogen bond network involving polar residues in TMs 1, 2, 6 and 7 is postulated to play an integral role in receptor activation (Nygaard et al., 2010). Given the importance of TMs 6 and 7 for the transitioning of receptors into active conformations, these mode switches may be attributed to either a loss of an important direct contact that facilitates receptor activation upon modulator binding or a global (secondary) effect on protein conformations that prevents some modulators, but not others, from engendering active conformations.

Collectively, these findings highlight the subtleties of interactions within the common mGlu allosteric binding pocket that determine allosteric modulator affinity and cooperativity. The identification of point mutations that engender a molecular switch in PAM pharmacology

provides the first clues from the protein side of the equation as to the underlying determinants for this phenomenon. The prevalence of “molecular switches” raises concerns regarding metabolite pharmacology. A deeper understanding of the molecular basis of allosteric modulation has the potential to aid rational drug design efforts to predict and avoid undesirable pharmacology, including mode switches.

Acknowledgements

The authors would like to acknowledge Kristian W. Kauffman and Eric S. Dawson for their contribution to the comparative modeling of $mGlu_5$ and Colleen M. Niswender for critical reading of the manuscript.

Authorship Contributions

Participated in research design: Gregory, Stauffer, Nguyen, Meiler, Conn,

Conducted experiments: Gregory, Nguyen, Reiff, Squire

Contributed new reagents: Stauffer, Lindsley

Performed data analysis: Gregory, Nguyen, Reiff, Squire

Wrote or contributed to writing of manuscript: Gregory, Nguyen, Meiler, Conn,

References

Alexander N, Woetzel N and Meiler J (2011) Bcl: :Cluster: A method for clustering biological molecules coupled with visualization in the Pymol Molecular Graphics System, in *Proceedings of the 2011 IEEE 1st International Conference on Computational Advances in Bio and Medical Sciences* pp 13-18, IEEE Computer Society.

Ametamey SM, Treyer V, Streffer J, Wyss MT, Schmidt M, Blagoev M, Hintermann S, Auberson Y, Gasparini F, Fischer UC and Buck A (2007) Human PET studies of metabotropic glutamate receptor subtype 5 with 11C-ABP688. *J Nucl Med* **48**(2): 247-252.

Barak LS, Menard L, Ferguson SS, Colapietro AM and Caron MG (1995) The conserved seven-transmembrane sequence NP(X)2,3Y of the G-protein-coupled receptor superfamily regulates multiple properties of the beta 2-adrenergic receptor. *Biochemistry* **34**(47): 15407-15414.

Chen Y, Goudet C, Pin JP and Conn PJ (2008) N-{4-Chloro-2-[(1,3-dioxo-1,3-dihydro-2H-isoindol-2-yl)methyl]phenyl}-2-hydroxybe nzamide (CPPHA) acts through a novel site as a positive allosteric modulator of group 1 metabotropic glutamate receptors. *Mol Pharmacol* **73**(3): 909-918.

Chen Y, Nong Y, Goudet C, Hemstapat K, de Paulis T, Pin JP and Conn PJ (2007) Interaction of novel positive allosteric modulators of metabotropic glutamate receptor 5 with the negative allosteric antagonist site is required for potentiation of receptor responses. *Mol Pharmacol* **71**(5): 1389-1398.

Cheng Y and Prusoff WH (1973) Relationship between the inhibition constant (K1) and the concentration of inhibitor which causes 50 per cent inhibition (I50) of an enzymatic reaction. *Biochem Pharmacol* **22**(23): 3099-3108.

Cherezov V, Rosenbaum DM, Hanson MA, Rasmussen SG, Thian FS, Kobilka TS, Choi HJ, Kuhn P, Weis WI, Kobilka BK and Stevens RC (2007) High-resolution crystal structure of an engineered human beta2-adrenergic G protein-coupled receptor. *Science* **318**(5854): 1258-1265.

Christopoulos A (1998) Assessing the distribution of parameters in models of ligand-receptor interaction: to log or not to log. *Trends Pharmacol Sci* **19**(9): 351-357.

Cosford ND, Tehrani L, Roppe J, Schweiger E, Smith ND, Anderson J, Bristow L, Brodkin J, Jiang X, McDonald I, Rao S, Washburn M and Varney MA (2003) 3-[(2-Methyl-1,3-thiazol-4-yl)ethynyl]-pyridine: a potent and highly selective metabotropic glutamate subtype 5 receptor antagonist with anxiolytic activity. *J Med Chem* **46**(2): 204-206.

Davis IW and Baker D (2009) RosettaLigand docking with full ligand and receptor flexibility. *J Mol Biol* **385**(2): 381-392.

Fritze O, Filipek S, Kuksa V, Palczewski K, Hofmann KP and Ernst OP (2003) Role of the conserved NPxxY(x)5,6F motif in the rhodopsin ground state and during activation. *Proc Natl Acad Sci U S A* **100**(5): 2290-2295.

Fukuda J, Suzuki G, Kimura T, Nagatomi Y, Ito S, Kawamoto H, Ozaki S and Ohta H (2009) Identification of a novel transmembrane domain involved in the negative modulation of mGluR1 using a newly discovered allosteric mGluR1 antagonist, 3-cyclohexyl-5-fluoro-6-methyl-7-(2-morpholin-4-ylethoxy)-4H-chromen-4-one. *Neuropharmacology* **57**(4): 438-445.

Gasparini F, Lingenhohl K, Stoehr N, Flor PJ, Heinrich M, Vranesic I, Biollaz M, Allgeier H, Heckendorn R, Urwyler S, Varney MA, Johnson EC, Hess SD, Rao SP, Sacaan AI, Santori EM, Velicelebi G and Kuhn R (1999) 2-Methyl-6-(phenylethynyl)-pyridine (MPEP), a potent, selective and systemically active mGlu5 receptor antagonist. *Neuropharmacology* **38**(10): 1493-1503.

Gregory KJ, Dong EN, Meiler J and Conn PJ (2011) Allosteric modulation of metabotropic glutamate receptors: structural insights and therapeutic potential. *Neuropharmacology* **60**(1): 66-81.

Gregory KJ, Noetzel MJ, Rook JM, Vinson PN, Stauffer SR, Rodriguez AL, Emmitte KA, Zhou Y, Chun AC, Felts AS, Chauder BA, Lindsley CW, Niswender CM and Conn PJ (2012) Investigating mGlu5 Allosteric Modulator Cooperativity, Affinity and Agonism: Enriching Structure-function Studies and Structure-activity Relationships. *Mol Pharmacol* **82**(5): 860-75.

Hammond AS, Rodriguez AL, Townsend SD, Niswender CM, Gregory KJ, Lindsley CW and Conn PJ (2010) Discovery of a Novel Chemical Class of mGlu(5) Allosteric Ligands with Distinct Modes of Pharmacology. *ACS Chem Neurosci* **1**(10): 702-716.

Holst B, Nygaard R, Valentin-Hansen L, Bach A, Engelstoft MS, Petersen PS, Frimurer TM and Schwartz TW (2010) A conserved aromatic lock for the tryptophan rotameric switch in TM-VI of seven-transmembrane receptors. *J Biol Chem* **285**(6): 3973-3985.

Honer M, Stoffel A, Kessler LJ, Schubiger PA and Ametamey SM (2007) Radiolabeling and in vitro and in vivo evaluation of [18F]-FE-DABP688 as a PET radioligand for the metabotropic glutamate receptor subtype 5. *Nucl Med Biol* **34**(8): 973-980.

Kinney GG, O'Brien JA, Lemaire W, Burno M, Bickel DJ, Clements MK, Chen TB, Wisnoski DD, Lindsley CW, Tiller PR, Smith S, Jacobson MA, Sur C, Duggan ME, Pettibone DJ, Conn PJ and Williams DL, Jr. (2005) A novel selective positive allosteric modulator of metabotropic glutamate receptor subtype 5 has in vivo activity and antipsychotic-like effects in rat behavioral models. *J Pharmacol Exp Ther* **313**(1): 199-206.

Knoflach F, Mutel V, Jolidon S, Kew JN, Malherbe P, Vieira E, Wichmann J and Kemp JA (2001) Positive allosteric modulators of metabotropic glutamate 1 receptor: characterization, mechanism of action, and binding site. *Proc Natl Acad Sci U S A* **98**(23): 13402-13407.

Lamb JP, Engers DW, Niswender CM, Rodriguez AL, Venable DF, Conn PJ and Lindsley CW (2011) Discovery of molecular switches within the ADX-47273 mGlu5 PAM scaffold that modulate modes of pharmacology to afford potent mGlu5 NAMs, PAMs and partial antagonists. *Bioorg Med Chem Lett* **21**(9): 2711-2714.

Lazareno S and Birdsall N (1995) Detection, quantitation, and verification of allosteric interactions of agents with labeled and unlabeled ligands at G protein-coupled receptors: interactions of strychnine and acetylcholine at muscarinic receptors. *Mol Pharmacol* **48**(2): 362-378.

Leach K, Sexton PM and Christopoulos A (2007) Allosteric GPCR modulators: taking advantage of permissive receptor pharmacology. *Trends Pharmacol Sci* **28**(8): 382-389.

Leaver-Fay A, Tyka M, Lewis SM, Lange OF, Thompson J, Jacak R, Kaufman K, Renfrew PD, Smith CA, Sheffler W, Davis IW, Cooper S, Treuille A, Mandell DJ, Richter F, Ban YE, Fleishman SJ, Corn JE, Kim DE, Lyskov S, Berrondo M, Mentzer S, Popovic Z, Havranek JJ, Karanicolas J, Das R, Meiler J, Kortemme T, Gray JJ, Kuhlman B, Baker D

and Bradley P (2011) ROSETTA3: an object-oriented software suite for the simulation and design of macromolecules. *Methods Enzymol* **487**: 545-574.

Lemmon G and Meiler J (2012) Rosetta Ligand docking with flexible XML protocols. *Methods Mol Biol* **819**: 143-155.

Liu F, Grauer S, Kelley C, Navarra R, Graf R, Zhang G, Atkinson PJ, Popiolek M, Wantuch C, Khawaja X, Smith D, Olsen M, Kouranova E, Lai M, Pruthi F, Pulicicchio C, Day M, Gilbert A, Pausch MH, Brandon NJ, Beyer CE, Comery TA, Logue S, Rosenzweig-Lipson S and Marquis KL (2008) ADX47273 [S-(4-fluoro-phenyl)-{3-[3-(4-fluoro-phenyl)-[1,2,4]-oxadiazol-5-yl]-piperidin-1- yl}-methanone]: a novel metabotropic glutamate receptor 5-selective positive allosteric modulator with preclinical antipsychotic-like and procognitive activities. *J Pharmacol Exp Ther* **327**(3): 827-839.

Malherbe P, Kratochwil N, Muhlemann A, Zenner M-T, Fischer C, Stahl M, Gerber PR, Jaeschke G and Porter RHP (2006) Comparison of the binding pockets of two chemically unrelated allosteric antagonists of the mGlu5 receptor and identification of crucial residues involved in the inverse agonism of MPEP. *J Neurochem* **98**(2): 601-615.

Malherbe P, Kratochwil N, Zenner MT, Piussi J, Diener C, Kratzeisen C, Fischer C and Porter RH (2003) Mutational analysis and molecular modeling of the binding pocket of the metabotropic glutamate 5 receptor negative modulator 2-methyl-6-(phenylethynyl)-pyridine. *Mol Pharmacol* **64**(4): 823-832.

Manka JT, Vinson PN, Gregory KJ, Zhou Y, Williams R, Gogi K, Days E, Jadhav S, Herman EJ, Lavreysen H, Mackie C, Bartolome JM, Macdonald GJ, Steckler T, Daniels JS, Weaver CD, Niswender CM, Jones CK, Conn PJ, Lindsley CW and Stauffer SR (2012) Optimization of an ether series of mGlu(5) positive allosteric modulators: Molecular

determinants of MPEP-site interaction crossover. *Bioorg Med Chem Lett* **22**(20): 6481-6485.

Meiler J and Baker D (2006) ROSETTALIGAND: protein-small molecule docking with full side-chain flexibility. *Proteins* **65**(3): 538-548.

Melancon BJ, Hopkins CR, Wood MR, Emmitte KA, Niswender CM, Christopoulos A, Conn PJ and Lindsley CW (2012) Allosteric modulation of seven transmembrane spanning receptors: theory, practice, and opportunities for central nervous system drug discovery. *J Med Chem* **55**(4): 1445-1464.

Miedlich SU, Gama L, Seuwen K, Wolf RM and Breitwieser GE (2004) Homology modeling of the transmembrane domain of the human calcium sensing receptor and localization of an allosteric binding site. *J Biol Chem* **279**(8): 7254-7263.

Molck C, Harpsoe K, Gloriam DE, Clausen RP, Madsen U, Pedersen LO, Jimenez HN, Nielsen SM, Mathiesen JM and Brauner-Osborne H (2012) Pharmacological Characterization and Modeling of the Binding Sites of Novel 1,3-bis(pyridinylethynyl)benzenes as Metabotropic Glutamate Receptor 5-selective Negative Allosteric Modulators. *Mol Pharmacol* **82**(5):929-37.

Muhlemann A, Ward NA, Kratochwil N, Diener C, Fischer C, Stucki A, Jaeschke G, Malherbe P and Porter RH (2006) Determination of key amino acids implicated in the actions of allosteric modulation by 3,3'-difluorobenzaldazine on rat mGlu5 receptors. *Eur J Pharmacol* **529**(1-3): 95-104.

Niswender CM and Conn PJ (2010) Metabotropic glutamate receptors: physiology, pharmacology, and disease. *Annu Rev Pharmacol Toxicol* **50**: 295-322.

Noetzel MJ, Rook JM, Vinson PN, Cho HP, Days E, Zhou Y, Rodriguez AL, Lavreysen H, Stauffer SR, Niswender CM, Xiang Z, Daniels JS, Jones CK, Lindsley CW, Weaver CD and Conn PJ (2012) Functional impact of allosteric agonist activity of selective positive allosteric modulators of metabotropic glutamate receptor subtype 5 in regulating central nervous system function. *Mol Pharmacol* **81**(2): 120-133.

Nygaard R, Valentin-Hansen L, Mokrosinski J, Frimurer TM and Schwartz TW (2010) Conserved water-mediated hydrogen bond network between TM-I, -II, -VI, and -VII in 7TM receptor activation. *J Biol Chem* **285**(25): 19625-19636.

O'Brien JA, Lemaire W, Chen TB, Chang RS, Jacobson MA, Ha SN, Lindsley CW, Schaffhauser HJ, Sur C, Pettibone DJ, Conn PJ and Williams DL, Jr. (2003) A family of highly selective allosteric modulators of the metabotropic glutamate receptor subtype 5. *Mol Pharmacol* **64**(3): 731-740.

O'Brien JA, Lemaire W, Wittmann M, Jacobson MA, Ha SN, Wisnoski DD, Lindsley CW, Schaffhauser HJ, Rowe B, Sur C, Duggan ME, Pettibone DJ, Conn PJ and Williams DL, Jr. (2004) A novel selective allosteric modulator potentiates the activity of native metabotropic glutamate receptor subtype 5 in rat forebrain. *J Pharmacol Exp Ther* **309**(2): 568-577.

Pagano A, Ruegg D, Litschig S, Stoehr N, Stierlin C, Heinrich M, Floersheim P, Prezeau L, Carroll F, Pin JP, Cambria A, Vranesic I, Flor PJ, Gasparini F and Kuhn R (2000) The non-competitive antagonists 2-methyl-6-(phenylethynyl)pyridine and 7-hydroxyiminocyclopropan[b]chromen-1a-carboxylic acid ethyl ester interact with overlapping binding pockets in the transmembrane region of group I metabotropic glutamate receptors. *J Biol Chem* **275**(43): 33750-33758.

Prioleau C, Visiers I, Ebersole BJ, Weinstein H and Sealfon SC (2002) Conserved helix 7 tyrosine acts as a multistate conformational switch in the 5HT2C receptor. Identification of a novel "locked-on" phenotype and double revertant mutations. *J Biol Chem* **277**(39): 36577-36584.

Rodriguez AL, Grier MD, Jones CK, Herman EJ, Kane AS, Smith RL, Williams R, Zhou Y, Marlo JE, Days EL, Blatt TN, Jadhav S, Menon UN, Vinson PN, Rook JM, Stauffer SR, Niswender CM, Lindsley CW, Weaver CD and Conn PJ (2010) Discovery of novel allosteric modulators of metabotropic glutamate receptor subtype 5 reveals chemical and functional diversity and in vivo activity in rat behavioral models of anxiolytic and antipsychotic activity. *Mol Pharmacol* **78**(6): 1105-1123.

Rodriguez AL, Nong Y, Sekaran NK, Alagille D, Tamagnan GD and Conn PJ (2005) A close structural analog of 2-methyl-6-(phenylethynyl)-pyridine acts as a neutral allosteric site ligand on metabotropic glutamate receptor subtype 5 and blocks the effects of multiple allosteric modulators. *Mol Pharmacol* **68**(6): 1793-1802.

Rodriguez AL, Williams R, Zhou Y, Lindsley SR, Le U, Grier MD, Weaver CD, Conn PJ and Lindsley CW (2009) Discovery and SAR of novel mGluR5 non-competitive antagonists not based on an MPEP chemotype. *Bioorg Med Chem Lett* **19**(12): 3209-3213.

Sharma S, Kedrowski J, Rook JM, Smith RL, Jones CK, Rodriguez AL, Conn PJ and Lindsley CW (2009) Discovery of molecular switches that modulate modes of metabotropic glutamate receptor subtype 5 (mGlu5) pharmacology in vitro and in vivo within a series of functionalized, regioisomeric 2- and 5-(phenylethynyl)pyrimidines. *J Med Chem* **52**(14): 4103-4106.

Sheffler DJ, Wenthur CJ, Bruner JA, Carrington SJS, Vinson PN, Gogi KK, Blobaum AL, Morrison RD, Vamos M, Cosford NDP, Stauffer SR, Scott Daniels J, Niswender CM, Jeffrey Conn P and Lindsley CW (2012) Development of a novel, CNS-penetrant, metabotropic glutamate receptor 3 (mGlu3) NAM probe (ML289) derived from a closely related mGlu5 PAM. *Bioorg Med Chem Lett* **22**(12): 3921-3925.

Shi L, Liapakis G, Xu R, Guarnieri F, Ballesteros JA and Javitch JA (2002) Beta2 adrenergic receptor activation. Modulation of the proline kink in transmembrane 6 by a rotamer toggle switch. *J Biol Chem* **277**(43): 40989-40996.

Suzuki G, Kimura T, Satow A, Kaneko N, Fukuda J, Hikichi H, Sakai N, Maehara S, Kawagoe-Takaki H, Hata M, Azuma T, Ito S, Kawamoto H and Ohta H (2007) Pharmacological characterization of a new, orally active and potent allosteric metabotropic glutamate receptor 1 antagonist, 4-[1-(2-fluoropyridin-3-yl)-5-methyl-1H-1,2,3-triazol-4-yl]-N-isopropyl-N-methyl- 3,6-dihydropyridine-1(2H)-carboxamide (FTIDC). *J Pharmacol Exp Ther* **321**(3): 1144-1153.

Treyer V, Streffer J, Wyss MT, Bettio A, Ametamey SM, Fischer U, Schmidt M, Gasparini F, Hock C and Buck A (2007) Evaluation of the metabotropic glutamate receptor subtype 5 using PET and 11C-ABP688: assessment of methods. *J Nucl Med* **48**(7): 1207-1215.

Varney MA, Cosford ND, Jachec C, Rao SP, Sacaan A, Lin FF, Bleicher L, Santori EM, Flor PJ, Allgeier H, Gasparini F, Kuhn R, Hess SD, Velicelebi G and Johnson EC (1999) SIB-1757 and SIB-1893: selective, noncompetitive antagonists of metabotropic glutamate receptor type 5. *J Pharmacol Exp Ther* **290**(1): 170-181.

Visiers I, Ballesteros JA and Weinstein H (2002) Three-dimensional representations of G protein-coupled receptor structures and mechanisms. *Methods Enzymol* **343**: 329-371.

Wood MR, Hopkins CR, Brogan JT, Conn PJ and Lindsley CW (2011) "Molecular switches" on mGluR allosteric ligands that modulate modes of pharmacology. *Biochemistry* **50**(13): 2403-2410.

Yanagawa M, Yamashita T and Shichida Y (2009) Activation switch in the transmembrane domain of metabotropic glutamate receptor. *Mol Pharmacol* **76**(1): 201-207.

Yarov-Yarovoy V, Schonbrun J and Baker D (2006) Multipass membrane protein structure prediction using Rosetta. *Proteins* **62**(4): 1010-1025.

Zhao Z, Wisnoski DD, O'Brien JA, Lemaire W, Williams DL, Jr., Jacobson MA, Wittman M, Ha SN, Schaffhauser H, Sur C, Pettibone DJ, Duggan ME, Conn PJ, Hartman GD and Lindsley CW (2007) Challenges in the development of mGluR5 positive allosteric modulators: the discovery of CPPHA. *Bioorg Med Chem Lett* **17**(5): 1386-1391.

Zhou Y, Manka JT, Rodriguez AL, Weaver CD, Days EL, Vinson PN, Jadhav S, Hermann EJ, Jones CK, Conn PJ, Lindsley CW and Stauffer SR (2010) Discovery of N-Aryl Piperazines as Selective mGluR5 Potentiators with Improved In Vivo Utility. *ACS Med Chem Lett* **1**(8): 433-438.

Footnotes

a) This work is supported by the National Institute of Mental Health [Grant 2R01 MH062646-13]; National Institute of Neurological Disorders and Stroke [Grant 2R01NS031373-16A2]; National Institute of Drug Abuse [Grant 1R01DA023947]; and Molecular Libraries Probe Production Centers Network [Grant 5 u54 MH84659-03, 5 u54 MH84659-03S1]. Karen J. Gregory is a recipient of a National Alliance for Research on Schizophrenia and Depression (NARSAD)-Maltz Young Investigator Award, an American Australian Association Merck Foundation Fellowship and a National Health and Medical Research Council (Australia) Overseas Biomedical Postdoctoral Training Fellowship. Work in the Meiler laboratory is supported through the National Institutes of Health [R01 GM080403, R01 MH090192, R01 GM099842] and the National Science Foundation [Career 0742762].

b) PJC is a consultant for Seaside Therapeutic and receives research support from Seaside Therapeutics and Johnson and Johnson/Janssen Pharmaceutica.

c) Reprint Requests should be addressed to P. Jeffrey Conn, Department of Pharmacology & Vanderbilt Center for Neuroscience Drug Discovery, Vanderbilt University Medical Center, 1215 Light Hall, 2215-B Garland Ave, Nashville, TN, USA, 37232-0697; jeff.conn@vanderbilt.edu

Figure legends

Figure 1. Probing the common allosteric binding site on $mGlu_5$ with negative allosteric modulator, MPEP.

A) At the wildtype rat $mGlu_5$ receptor, MPEP inhibits glutamate-mediated mobilization of intracellular Ca^{2+}, depressing the maximal response. B) Single point mutations of $mGlu_5$ were screened for their ability to impact inhibition of the maximal response to glutamate in the presence of 10nM MPEP. C) Comparison of MPEP affinity estimates at mutants with wildtype. Data represent the mean ± S.E.M of 3-6 experiments performed in duplicate. Error bars not shown lie within the dimensions of the symbol.

Figure 2. At two point mutations, MPEP did not fully depress the maximal response to glutamate.

MPEP inhibition of glutamate-mediated mobilization of intracellular Ca^{2+} at $mGlu_5$-P654F (A) and W784A (B). In the presence of MPEP at concentrations up to 100 uM, glutamate retained some activity in both cell lines. Data represent the mean ± S.E.M of 3-5 experiments performed in duplicate. Error bars not shown lie within the dimensions of the symbol.

Figure 3. The negative allosteric modulator MPEP docked into $mGlu_5$ comparative model.

MPEP was docked into the $mGlu_5$ comparative model in two separate experiments, centered at P654 and S808. (A) The lowest energy conformation for MPEP from the largest cluster docked at P654 is shown in green and at S808 is shown in cyan. Highlighted are the residues that caused decreases in MPEP affinity when mutated, colored by graded effect compared to wildtype. (B) The lowest energy models from the largest three clusters for MPEP docked at P654. (C) The lowest energy models from the largest five clusters for MPEP docked at S808. Predicted

hydrogen bonds between the nitrogen on the pyridine ring and S808 are depicted by dotted blue lines.

Figure 4. Potentiation of glutamate-mediated Ca^{2+} mobilization by nicotinamide and picolinamide acetylene PAMs at wildtype $mGlu_5$.

The six PAMs included in this study potentiate the response to glutamate at $mGlu_5$-wildtype in a Ca^{++} mobilization assay with varying degrees of cooperativity, as evidenced by increased glutamate potencies in the presence of PAMs. Nicotinamide acetylene PAMs are shown on the left (A, B, C), with the corresponding picolinamide acetylene PAM on the right (D, E, F). Data represent the mean ± S.E.M of 3-7 experiments performed in duplicate. Error bars not shown lie within the dimensions of the symbol.

Figure 5. Effect of mutations on the fold-shift caused by a single concentration of PAM

Nicotinamide acetylene PAMs are shown on the left, with the corresponding picolinamide acetylene PAM on the left as indicated. The increase in glutamate potency in the presence of PAM, or fold-shift, at each mutant is expressed relative to that observed for the same concentration at the wildtype receptor. Specifically, PAM concentrations used were: 10 μM VU0360173; 1 μM VU0360172; 100 nM VU0415051; 100 nM VU0405398; 10 nM VU0403602; and 10 nM VU0405386. # denotes no detectable PAM activity. * denotes significantly different to wildtype, $p<0.05$, one-way ANOVA, Dunnett's post-test. Data represent the mean ± S.E.M of 3-7 experiments performed in duplicate. Error bars not shown lie within the dimensions of the symbol.

Figure 6. Effect of mutations on positive allosteric modulator affinity estimates.

Nicotinamide acetylene PAMs are shown in the top three panels (A, B, C), with the corresponding picolinamide acetylene PAM in the bottom three panels (D, E, F). Affinity

estimates (pK_B) were derived using an operational model of allosterism (Gregory et al., 2012; Leach et al., 2007) from progressive fold-shifts of the glutamate concentration-response curve for Ca^{2+} mobilization. The difference between the pK_B for the mutant versus wildtype is plotted. # denotes no detectable PAM activity. * denotes significantly different to wildtype, $p<0.05$, one-way ANOVA, Dunnett's post-test. Data represent the mean ± S.E.M of 3-7 experiments performed in duplicate. Error bars not shown lie within the dimensions of the symbol.

Figure 7. Computational docking of three pairs of nicotinamide and picolinamide acetylene positive allosteric modulators into $mGlu_5$. A) VU0360173 in blue and VU0405398 in green, B) VU0360172 in blue and VU0403602 in green and C) VU0415051 in blue and VU0405386 in green. Residues that when mutated caused a significant decrease in modulator affinity in $mGlu_5$ are highlighted in the respective color of the modulator. Residues that affect both the nicotinamide and picolinamde in the pair are highlighted in purple. A predicted hydrogen bond network involving the modulators, Y658, T780A and W784 is represented by the dashed black lines. Highlighted in grey are residues that influence the cooperativity of certain modulators.

Figure 8. Effect of mutations on positive allosteric modulator cooperativity factors.

Nicotinamide acetylene PAMs are shown in the top three panels (A, B, C), with the corresponding picolinamide acetylene PAM in the bottom three panels (D, E, F). Cooperativity estimates (logβ) were derived using an operational model of allosterism (Gregory et al., 2012; Leach et al., 2007) from progressive fold-shifts of the glutamate concentration-response curve for Ca^{2+} mobilization. The difference between the logβ for the mutant versus wildtype is plotted. # denotes no detectable PAM activity. * denotes significantly different to wildtype, $p<0.05$, one-way ANOVA, Dunnett's post-test. Data represent the mean ± S.E.M of 3-7 experiments performed in duplicate. Error bars not shown lie within the dimensions of the symbol.

Figure 9. Characterization of mutations that engender a molecular switch in PAM pharmacology

A) At $mGlu_5$-Y658V, 10 μM and 30 μM VU0405398 inhibited the response to maximal glutamate. B) The interaction between glutamate and VU0415051 at the T780A mutant is negative, with inhibition approaching a limit as defined by the cooperativity. C) At S808A, VU0405398 causes a reduction in glutamate potency and depresses the maximal response to glutamate. D) Concentration-response curves for VU0405398 inhibition of an ~EC_{80} of glutamate in the absence and presence of the indicated concentrations of VU0405386. E) Schild regression of the interaction between VU0405386 and VU0405398 at S808A. Data represent the mean ± S.E.M of 3-6 experiments performed in duplicate. Error bars not shown lie within the dimensions of the symbol.

Figure 10. Mutations engendering a molecular switch for $mGlu_5$ allosteric modulators. A) VU0405398 docked into wildtype $mGlu_5$ (green) and the S808A mutant (magenta). B) VU0415051 docked into wildtype $mGlu_5$ (blue) and the T780A mutant (magenta). C) VU0405386 docked into wildtype $mGlu_5$ (blue) and the S808A mutant (magenta). Mutated residues are colored by element. Key affinity determinants are highlighted to show conformational changes in the binding pocket.

Table 1: Equilibrium binding parameters for [^{3}H]methoxyPEPy and MPEP at mGlu$_5$ mutations. Data represent the mean ± s.e.m of a minimum of three independent determinations.

	[^{3}H]methoxyPEPy pK_D [a]	B_{max} [b] (pmol/mg)	MPEP pK_I [c]
R5-wt (low)	8.24 ± 0.09	0.6 ± 0.0*[#]	7.87 ± 0.04[#]
R5-wt (poly)	8.23 ± 0.10	3.8 ± 0.8	7.77 ±0.03
F585I	7.91 ± 0.19	1.8 ± 0.6	7.93 ± 0.09
R647A	8.22 ± 0.08	1.6 ± 1.3	n.d.
I650A	8.43 ± 0.11	1.0 ± 0.1*	8.34 ± 0.11*
G651F	No appreciable binding		
P654S	No appreciable binding		
P654F	No appreciable binding		
S657C	8.35 ± 0.28	0.8 ±0.3*	8.12 ±0.09
Y658V	No appreciable binding		
V739M	8.19 ± 0.02	1.6 ± 0.3	7.91 ± 0.07
P742S	7.71 ± 0.29	0.4 ± 0.2*	7.67 ± 0.14
L743V	7.92 ± 0.09	1.1 ± 0.2*	7.23 ± 0.10*
N746A	7.72 ± 0.05	1.2 ± 0.4*	7.60 ± 0.08
G747V	8.37 ± 0.07	1.9 ± 0.6	7.88 ± 0.06
T779A	8.17 ± 0.13	0.8 ± 0.2*	
T780A	No appreciable binding		
W784A	No appreciable binding		
V788A	8.13 ± 0.08	1.0 ± 0.3*	7.71 ± 0.13
F792A	8.11 ± 0.21	1.7 ± 0.6	7.90 ± 0.13
S806A	7.71 ± 0.07	1.2 ± 0.1*	7.21 ± 0.07*
S808A	No appreciable binding		
S808T	No appreciable binding		
A809V	No appreciable binding		
A809G	No appreciable binding		
T810A	7.86 ± 0.15	2.0 ± 0.4	7.28 ± 0.09*
C815A	8.00 ± 0.19	0.8 ± 0.1*	7.57 ± 0.02

* denotes significantly different to wild type (polyclonal) value, $p<0.05$, one-way ANOVA, Dunnett's post test.
n.d. denotes not determined.
[#] data previously reported (Gregory et al., 2012).
[a] negative logarithm of the equilibrium dissociation constant of [^{3}H]methoxyPEPy.
[b] maximal number of binding sites.
[c] negative logarithm of the equilibrium dissociation constant of MPEP.

Table 2: Affinity estimates (pK_I) for positive allosteric modulators at $mGlu_5$-wt and mutants from inhibition binding assays.

Data represent the mean ± s.e.m of a minimum of three independent determinations.

	VU0360172 (nicotinamide)	VU0403602 (picolinamide)	VU0360173 (nicotinamide)	VU0405398 (picolinamide)	VU0415051 (nicotinamide)	VU0405386 (picolinamide)
R5-wt (low)	6.57 ± 0.02[#]	8.26 ± 0.15	5.12 ± 0.07	6.05 ± 0.12[#]	6.88 ± 0.04[#]	7.98 ± 0.05[#]
I650A	n.d.	7.89 ± 0.10	5.30 ± 0.26	6.41 ± 0.14	6.62 ± 0.11	7.69 ± 0.15
P742S	5.90 ±0.12*	7.24 ± 0.23*	5.12 ± 0.27	5.78 ± 0.14	6.35 ± 0.13*	7.19 ± 0.12*
L743V	6.32 ± 0.06	6.98 ± 0.10*	4.86 ± 0.08	5.71 ± 0.01*	6.25 ± 0.17*	7.58 ± 0.04
N746A	6.22 ± 0.07	7.49 ± 0.07*	4.63 ± 0.10	5.75 ± 0.03	6.35 ± 0.26*	7.45 ± 0.30
G747V	6.76 ± 0.05	n.d.	n.d.	n.d.	7.06 ± 0.27	8.17 ± 0.35
V788A	7.08 ± 0.23	8.70 ± 0.02	6.10 ± 0.09*	7.87 ± 0.05*	8.15 ± 0.07*	9.20 ± 0.10*
F792A	7.06 ±0.15	7.85 ± 0.04	5.68 ± 0.06	6.74 ± 0.08*	7.09 ± 0.06	7.71 ± 0.19
C815A	6.74 ± 0.24	8.01 ± 0.03	5.01 ± 0.07	6.26 ± 0.04	6.92 ± 0.11	7.96 ± 0.16

* denotes significantly different to value at wild type receptor, $p<0.05$, one-way ANOVA, with Dunnett's post test.
n.d. indicates not determined
[#] data previously reported (Gregory et al., 2012)

Table 3: Affinity estimates (pK_B) for allosteric modulators at $mGlu_5$-wt and mutants derived from operational model analysis of interactions with glutamate. Data represent mean ± s.e.m from 4-8 independent experiments performed in duplicate.

	MPEP	VU0360172 (nicotinamide)	VU0403602 (picolinamide)	VU0360173 (nicotinamide)	VU0405398 (picolinamide)	VU0415051 (nicotinamide)	VU0405386 (picolinamide)
R5-wt (poly)	8.58 ± 0.17[#]	6.68 ± 0.15	8.13 ± 0.26	5.45 ± 0.27	6.94 ± 0.17	7.34 ± 0.18	8.04 ± 0.26
R647A	8.89 ± 0.19	6.29 ± 0.12	7.99 ± 0.09	4.91 ± 0.14	6.94 ± 0.10	7.28 ± 0.25	7.74 ± 0.12
I650A	8.62 ± 0.03	7.12 ± 0.19	7.97 ± 0.13	n.d.	7.29 ± 0.15	n.d.	8.10 ± 0.15
G651F	7.53 ± 0.18*	5.86 ± 0.18*	6.50 ± 0.18*	No PAM	5.99 ± 0.28*	6.94 ± 0.19	7.14 ± 0.08
P654S	7.10 ± 0.06*	6.39 ± 0.24	7.33 ± 0.16	<5	5.80 ± 0.27*	5.69 ± 0.46*	7.81 ± 0.27
P654F	4.11 ± 0.21*	5.91 ± 0.17	5.99 ± 0.26*	No PAM	5.33 ± 0.27*	5.25 ± 0.19*	6.23 ± 0.22*
S657C	8.32 ± 0.08	n.d.	7.41 ± 0.17	n.d.	6.99 ± 0.31	6.78 ± 0.12	7.68 ± 0.06
Y658V	6.57 ± 0.13[#]*	No PAM	No PAM	No PAM	4.97 ± 0.35*	No PAM	No PAM
P742S	8.07 ± 0.17*	6.57 ± 0.10	7.50 ± 0.12	4.65 ± 0.17	6.83 ± 0.20	7.09 ± 0.04	7.96 ± 0.16
L743V	8.04 ± 0.10[#]*	6.97 ± 0.15	7.93± 0.14	5.46 ± 0.12	6.77 ± 0.11	7.75 ± 0.20	8.36 ± 0.10
N746A	8.30 ± 0.06	6.66 ± 0.10	7.99 ± 0.11	n.d.	6.50 ± 0.23	n.d.	8.06 ± 0.17
T780A	7.36 ± 0.02*	No PAM	6.03 ± 0.13*	No PAM	5.59 ± 0.05*	5.82 ± 0.40*	5.32 ± 0.24*
W784A	5.50 ± 0.29*	6.76 ± 0.14	7.09 ± 0.34*	5.03 ± 0.44	6.23 ± 0.20	7.14 ± 0.15	7.53 ± 0.14
V788A	7.89 ± 0.13*	7.28 ± 0.17	8.43 ± 0.20	6.28 ± 0.18	7.84 ± 0.14	8.07 ± 0.19	8.79 ± 0.08
F792A	8.93 ± 0.04	7.25 ± 0.33	8.03 ± 0.02	4.80 ± 0.20	7.34 ± 0.20	8.06 ± 0.24	7.02 ± 0.47*
S806A	8.36 ± 0.06	n.d.	n.d.	n.d.	n.d.	n.d.	7.29 ± 0.45
S808A	6.98 ± 0.18*	6.15 ± 0.30	6.47 ± 0.10*	No PAM	6.28 ± 0.09	7.20 ± 0.44	7.48 ±0.20
S808T	6.90 ± 0.06*	6.59 ± 0.20	7.15 ± 0.33*	5.04 ± 0.33	6.40 ± 0.23	6.36 ± 0.26*	8.05 ± 0.27
A809V	6.52 ± 0.12[#]*	5.64 ± 0.19*	6.52 ± 0.21*	No PAM	No PAM	5.56 ± 0.12*	6.22 ± 0.14*
A809G	7.18 ± 0.04*	5.93 ± 0.18	6.59 ± 0.05*	5.13 ± 0.13	5.88 ± 0.05*	6.28 ± 0.11*	6.60 ± 0.24*
C815A	8.35 ± 0.05	6.58 ± 0.22	7.29 ± 0.26*	4.81 ± 0.13	6.73 ± 0.35	7.26 ± 0.11	7.63 ± 0.15

n.d. denotes not determined

"No PAM" indicates no observed positive allosteric modulation.

* denotes significantly different from wild type value, $p<0.05$, one-way ANOVA, Dunnett's post-test.

[#] data previously reported (Gregory et al., 2012Gregory et al., 2012).

Table 4: Functional cooperativity factors (logβ) for allosteric modulators at $mGlu_5$-wt and mutants derived from operational model analysis of interactions with glutamate. Data represent mean ± s.e.m from 4-8 independent experiments performed in duplicate.

	VU0360172 (nicotinamide)	VU0403602 (picolinamide)	VU0360173 (nicotinamide)	VU0405398 (picolinamide)	VU0415051 (nicotinamide)	VU0405386 (picolinamide)
R5-wt (poly)	0.37 ± 0.05	0.61 ± 0.08	0.17 ± 0.04	0.37 ± 0.04	0.40 ± 0.02	0.55 ± 0.07
R647A	0.44 ± 0.13	0.60 ± 0.09	0.26 ± 0.03	0.38 ± 0.05	0.41 ±0.11	0.58 ± 0.06
I650A	0.58 ± 0.05	0.55 ± 0.08	n.d.	0.51 ± 0.08	n.d.	0.56 ± 0.08
G651F	0.54 ± 0.07	0.79 ± 0.05	No PAM	0.43 ± 0.04	0.32 ± 0.05	0.70 ± 0.07
P654S	0.26 ± 0.01	0.56 ± 0.05	<5	0.34 ± 0.08	0.22 ± 0.10	0.32 ± 0.05
P654F	0.25 ± 0.04	0.58 ± 0.14	No PAM	0.17 ± 0.04	0.66 ± 0.09*	0.53 ± 0.09
S657C	n.d.	0.82 ± 0.15	n.d.	0.43 ± 0.15	0.55 ± 0.01	0.56 ± 0.12
Y658V	No PAM	No PAM	No PAM	NAM	No PAM	No PAM
P742S	0.87 ±0.10*	1.23 ± 0.06*	0.69 ± 0.07*	0.70 ± 0.15	0.92 ± 0.08*	1.12 ± 0.17*
L743V	0.36 ± 0.14	0.60 ± 0.06	0.43 ± 0.03	0.54 ± 0.08	0.36 ± 0.04	0.80 ± 0.03
N746A	0.62 ± 0.04	0.67 ± 0.04	n.d.	0.57 ± 0.05	n.d.	0.63 ± 0.02
T780A	No PAM	0.77 ± 0.08	No PAM	0.19 ± 0.01	-0.28 ± 0.02*	0.39 ± 0.04
W784A	0.90 ± 0.14*	1.05 ± 0.11*	0.41 ± 0.10	0.48 ± 0.09	0.88 ± 0.10*	0.66 ± 0.15
V788A	0.57 ± 0.10	0.68 ± 0.09	0.66 ± 0.12*	0.47 ± 0.05	0.53 ± 0.06	0.56 ± 0.11
F792A	0.66 ±0.12	0.97 ± 0.10	0.29 ± 0.11	0.73 ± 0.32	0.29 ± 0.02	0.85 ± 0.16
S806A	n.d.	n.d.	n.d.	n.d.	n.d.	0.79 ± 0.13
S808A	0.50 ± 0.06	0.57 ± 0.10*	No PAM	NAM	0.22 ± 0.02	neutral
S808T	0.46 ± 0.06	0.76 ± 0.12	0.28 ± 0.07	0.34 ± 0.04	0.41 ± 0.04	0.45 ± 0.06
A809V	0.60 ± 0.07	0.58 ± 0.09	No PAM	No PAM	0.37 ± 0.07	0.58 ± 0.11
A809G	0.55 ± 0.04	1.29 ± 0.07*	0.41 ± 0.07	0.70 ± 0.03	0.78 ± 0.12*	1.12 ± 0.17*
C815A	1.17 ± 0.12*	1.29 ± 0.10*	0.66 ± 0.06*	0.75 ± 0.24	0.86 ± 0.05*	1.38 ± 0.14*

n.d. denotes not determined

"No PAM" indicates no observed positive allosteric modulation.

* denotes significantly different from wild type value, $p<0.05$, one-way ANOVA, Dunnett's post-test.

A
peak response
(% glu max)
150
100
50
0
[MPEP]
0
1 nM
3 nM
10 nM
30 nM
100 nM
vehicle
-9
-8
-7
-6
-5
-4
log[glu] M
B
Effect of 10 nM MPEP on glu Emax
(% decrease)
100
50
0
R5wt
F585I
I650A
G651F
S653A
P654S
P654F
S657C
Y658V
V739M
P742S
L743V
N746A
G747V
T779A
T780A
I783A
W784A
V788A
F792A
S806A
S808T
A809V
A809G
T810A
A812S
L813A
C815A
M816A
C
Effect of mutations on MPEP pKB
(mutant pKB - wt pKB)
1
0
-1
-2
-3
-4
-5
R5wt
F585I
I650A
G651F
P654S
P654F
S657C
Y658V
P742S
L743V
N746A
G747V
T779A
T780A
W784A
V788A
F792A
S806A
S808A
S808T
A809V
A809G
T810A
C815A

Figure 1

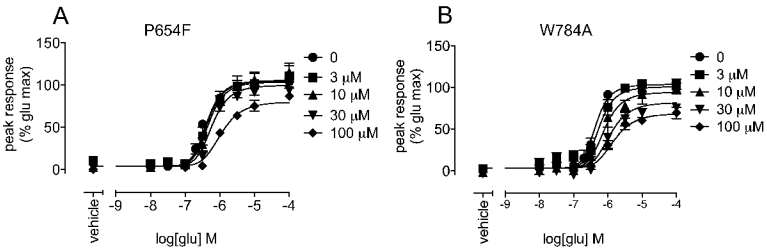
A
P654F
peak response
(% glu max)
150
100
50
0
vehicle
-9
-8
-7
-6
-5
-4
log[glu] M
0
3 μM
10 μM
30 μM
100 μM
B
W784A
peak response
(% glu max)
150
100
50
0
vehicle
-9
-8
-7
-6
-5
-4
log[glu] M
0
3 μM
10 μM
30 μM
100 μM

Figure 2

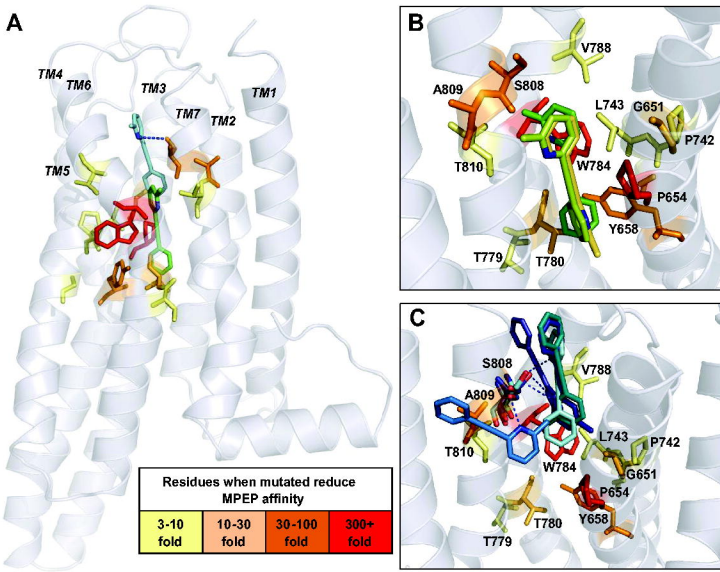
A
TM4
TM6
TM3
TM1
TM7
TM2
TM5
Residues when mutated reduce MPEP affinity
3-10 fold
10-30 fold
30-100 fold
300+ fold
B
V788
A809
S808
L743
G651
P742
T810
W784
P654
Y658
T779
T780
C
S808
V788
A809
T810
L743
P742
W784
G651
P654
T780
Y658
T779

Figure 3

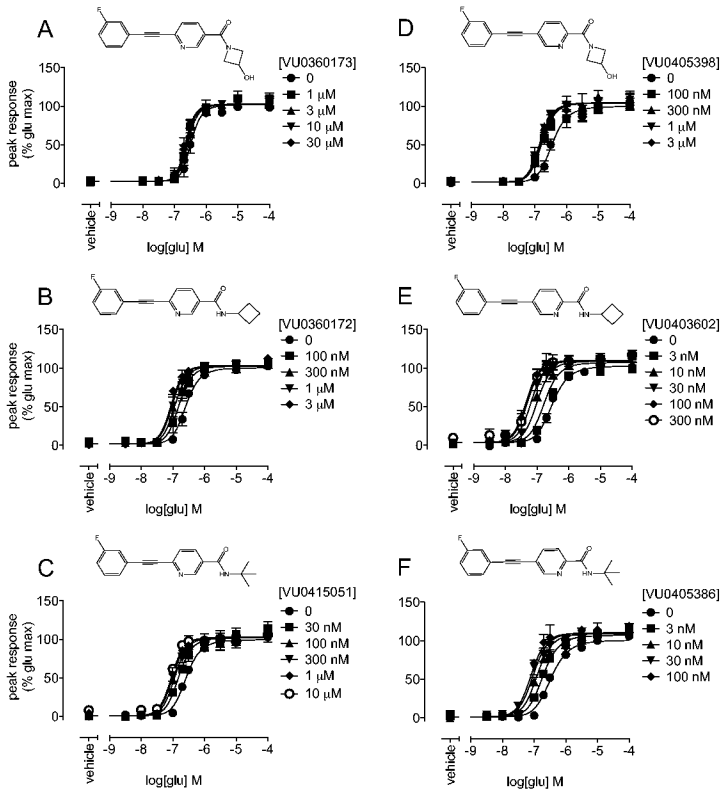
A
[VU0360173]
0
1 μM
3 μM
10 μM
30 μM
peak response
(% glu max)
log[glu] M
vehicle
B
[VU0360172]
0
100 nM
300 nM
1 μM
3 μM
C
[VU0415051]
0
30 nM
100 nM
300 nM
1 μM
10 μM
D
[VU0405398]
0
100 nM
300 nM
1 μM
3 μM
E
[VU0403602]
0
3 nM
10 nM
30 nM
100 nM
300 nM
F
[VU0405386]
0
3 nM
10 nM
30 nM
100 nM

Figure 4

A
VU0360173
B
VU0360172
C
VU0415051
D
VU0405398
E
VU0403602
F
VU0405386
Log[Fold shift at mutant / Fold shift at R5-wt]
Log[Fold shift at mutant / Fold shift at wild type]
F585H
R647A
I650A
G651F
S653A
P654A
P654F
S657C
Y758M
V739M
P742S
L743V
N746A
G747V
T780A
W784A
V788A
T791F
F792A
S806A
S808A
S808T
A809V
A809G
T810A
C815A

Figure 5

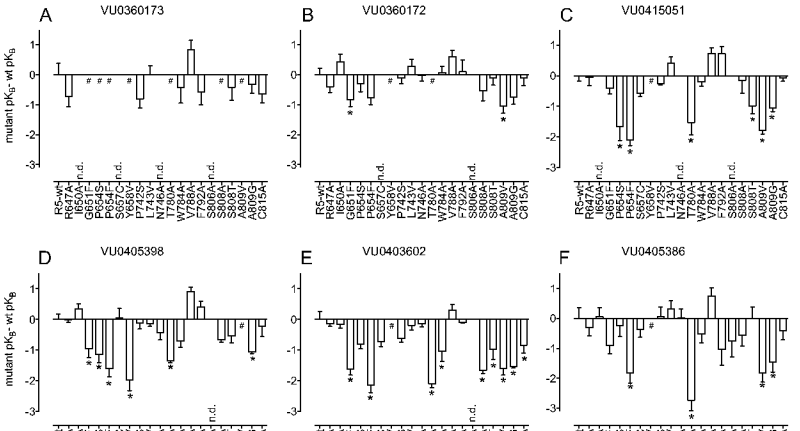
A
VU0360173
B
VU0360172
C
VU0415051
D
VU0405398
E
VU0403602
F
VU0405386
mutant pK_I - wt pK_I
mutant pK_B - wt pK_B
R5-wt
R647A
I650A
G651F
P654S
P654F
S657C
Y658V
P742S
L743V
N746A
T780A
W784A
V788A
F792A
S806A
S808A
S809T
A809V
A809G
C815A
n.d.

Figure 6

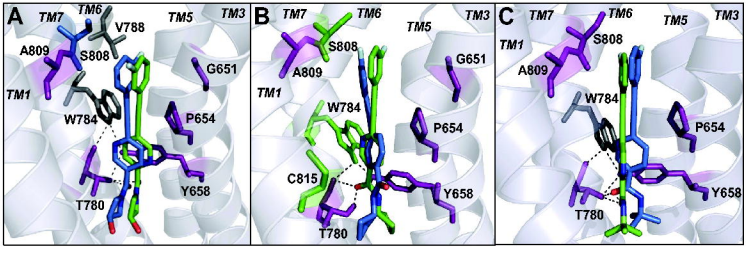
A
TM7
TM6
V788
TM5
TM3
A809
S808
G651
TM1
W784
P654
T780
Y658
B
TM7
TM6
TM5
TM3
S808
G651
A809
TM1
W784
P654
C815
Y658
T780
C
TM7
TM6
TM5
TM3
TM1
S808
A809
W784
P654
Y658
T780

Figure 7

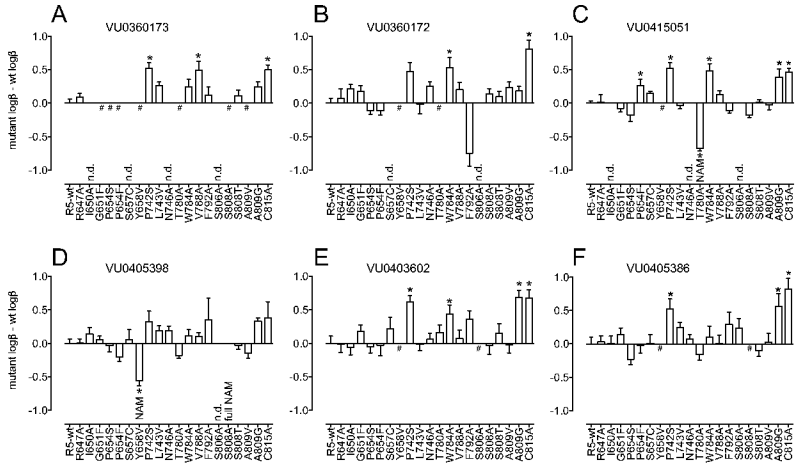
A
VU0360173
B
VU0360172
C
VU0415051
D
VU0405398
E
VU0403602
F
VU0405386
mutant logβ - wt logβ
1.0
0.5
0.0
-0.5
-1.0
n.d.
NAM ++
full NAM
R5-wt
R647A
I650A
G651F
P654S
P654F
S657C
Y658V
P742S
L743V
N746A
T780A
W784A
V788A
F792A
S806A
S808T
A809V
A809G
C815A

Figure 8

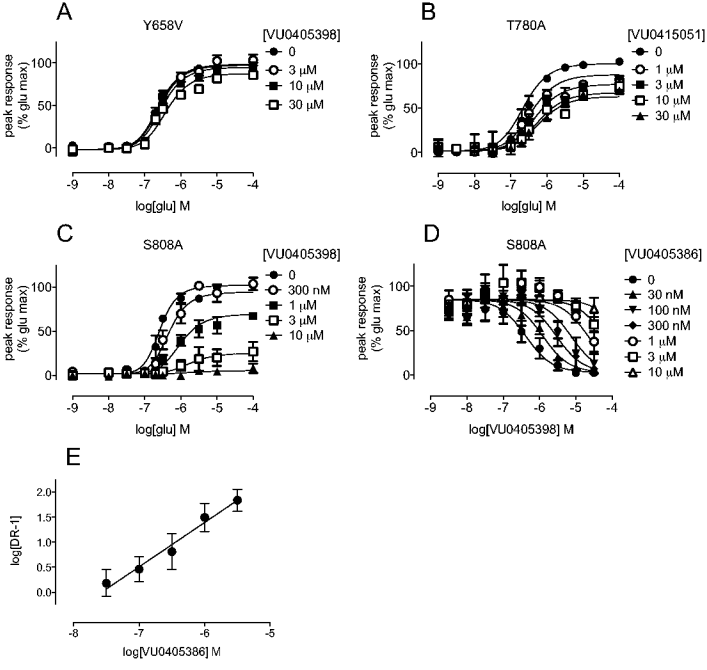
A
Y658V
[VU0405398]
0
3 μM
10 μM
30 μM
peak response
(% glu max)
log[glu] M
B
T780A
[VU0415051]
0
1 μM
3 μM
10 μM
30 μM
C
S808A
[VU0405398]
0
300 nM
1 μM
3 μM
10 μM
D
S808A
[VU0405386]
0
30 nM
100 nM
300 nM
1 μM
3 μM
10 μM
log[VU0405398] M
E
log[DR-1]
log[VU0405386] M

Figure 9

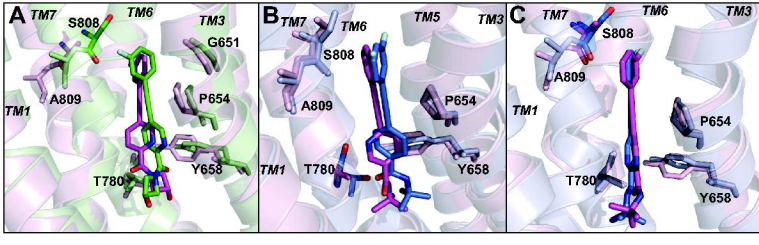
A
TM7
S808
TM6
TM3
G651
A809
TM1
P654
T780
Y658
B
TM7
TM6
TM5
TM3
S808
A809
P654
TM1
T780
Y658
C
TM7
TM6
TM3
S808
A809
TM1
P654
T780
Y658

Figure 10